The angular momentum dependence of nuclear optical potentials

Eur. Phys. J. A (2019) **55**: 147
DOI 10.1140/epja/i2019-12830-3

THE EUROPEAN PHYSICAL JOURNAL A

Review

The angular momentum dependence of nuclear optical potentials

R.S. Mackintosh[a]

School of Physical Sciences, The Open University, Milton Keynes, MK7 6AA, UK

Received: 15 April 2019 / Revised: 8 July 2019
Published online: 3 September 2019

Communicated by N. Alamanos

Abstract. The nuclear optical model potential (OMP) is generally assumed to be independent of the orbital angular momentum, l, of the interacting nuclei. Nucleon-nucleus and nucleus-nucleus interactions are customarily l independent in calculations of nuclear elastic scattering and in standard reaction codes. The evidence for various forms of l dependence of OMPs is reviewed and the importance of implementing these forms is evaluated. Existing arguments and evidence for l dependence are reviewed and new arguments and calculations are introduced. The relationship is examined between i) l dependence, and, ii) the undularity (waviness) of l-independent potentials that are S-matrix equivalent to l-dependent potentials. Such undularity is a property of the dynamic polarisation potential (DPP) generated by the coupling to reaction channels, or by coupling to excited states of the target or projectile nuclei. Various examples, particularly involving weakly bound projectile nuclei, are reviewed. Undularity is also a property of l-independent potentials that have been found in model-independent fits to precise, wide angular range, elastic scattering angular distributions; such undularity therefore indicates underlying l dependence. Cases of such phenomenological undularity, for both light and heavy ions, are referenced and shown to be related to undulatory properties of the dynamic polarisation potentials (DPPs) arising from channel coupling. Other forms of l dependence, that could be standard options in direct reaction codes, are also reviewed. The case is made that reaction-induced l dependence is a general property of nucleon-nucleus and nucleus-nucleus interactions and represents a valid extension of the nuclear optical model. A particular form of l dependence, parity dependence, arises due to the exchange of identical particles.

Contents

[a] e-mail: raymond.mackintosh@open.ac.uk

1 Introduction

The phenomenological optical model potential (OMP) for nucleon-nucleus and nucleus-nucleus scattering is almost always taken to be independent of the partial wave orbital angular momentum, l; for an early exception see ref. [1]. However there are both theoretical and phenomenological reasons to believe that some degree of l dependence is a general property of nuclear optical potentials. These reasons will be presented in what follows, along with a review of experimental and theoretical evidence for l dependence.

There are cases, mostly involving light nuclei, see sect. 8.1, where fully antisymmetrized calculations reveal strong and explicit l dependence, and these cases will be discussed. However the major concern of this review is with forms of l dependence for which the theoretical arguments are less direct. In the background throughout the review is a problem that arises in establishing l dependence on the basis of experimental results. This is that for any l-dependent potential there always exists an l-independent potential with the same complex S-matrix S_l (or S_{lj}). However, such an l-independent equivalent of an l-dependent potential will never have a smooth Woods-Saxon-like form, and is generally undulatory (wavy). It may also have radial regions where the imaginary component is emissive. The fact of two equivalent forms, each leading to identical calculated observables, is a complication for elastic scattering phenomenology and thus for attempts to develop a unified single-particle nucleon-nucleus interaction for both bound and scattering energies.

There are strong grounds for the l dependence of OMPs for nucleons and for composite projectile nuclei, from deuterons to ^{16}O, making angular momentum dependence a generic property of nucleon-nucleus and nucleus-nucleus interactions. Apart from its intrinsic interest, this must influence the analysis of direct reactions. Little is known concerning the effect of the l dependence of OMPs when they are applied in direct reactions, in contrast to the way that non-locality due to knock-on exchange is routinely compensated for.

For nucleons or other spin-$\frac{1}{2}$ projectiles, the l-independent equivalent of an l-dependent potential can be determined by applying $S_{lj} \rightarrow V(r) + \mathbf{l} \cdot \mathbf{s}\, V_{\rm SO}(r)$ inversion to the S_{lj} of the l-dependent potential. Inverting S_l for spin-zero projectiles is straightforward, and some cases of inversion for spin-1 have been carried out. Such S-matrix inversion will be referred to explicitly or implicitly at many points in this work and is the subject of sect. 4.

The l-independent equivalent of an l-dependent potential, will always be characterized by a certain degree of undularity (waviness). In fact undularity does occur in precision l-independent fits to high quality scattering data, and, furthermore, undularity can be shown to arise from channel coupling effects. This will be a recurrent theme in what follows. The relationship between l dependence and undularity is reviewed in more detail in ref. [2].

For nucleons and other light ions, there are global optical model potentials that describe elastic scattering data fairly well for a wide range of energies and target nuclei. For nucleons see [3], for deuterons see [4] and for mass-3 nuclei see [5]. Recently a theory-based global potential for nucleons of more than 40 MeV has appeared [6]. None of these global potentials include l dependence. Such global potentials, which fit a lot of data fairly well, leave plenty of scope for l dependence of potentials that precisely fit scattering data for each case. Such precise fits to data illuminate two aspects of elastic scattering: i) the manner in which departures of more exact fits from the global fit depend upon the properties of the target nucleus, and, ii) the occurrence and nature of l dependence. As will become apparent, these two are closely connected. The important point is that the difference between a fit for which $\chi^2/F \sim 1$, and a "*good fit*" as commonly described, is a generally untapped source of information, including evidence for l dependence. One theme of this review is what might be learned from precise fits to elastic scattering data; for a general discussion of this topic see ref. [7].

Historically, the possibility of a potential model description of nuclear scattering was for long considered implausible. When it was found that very simple models [8, 9] could account for much data in an approximate way, it became clear, see *e.g.* [10], that those simple models represented important understanding. However, although much better fits to data have become possible, there has been little motivation to extract all the information that might exist in precise, wide angular range, elastic scattering data. This is in contrast to the precise charge densities that have been extracted from elastic electron scattering data; however nuclear charge density is much less a model concept than the nuclear OMP. Almost all nuclear elastic scattering data is incomplete, in more ways than one, as will be made explicit with examples. Where precision OMP fits to relatively complete data have been accomplished, undulatory potentials have emerged. Such undularity lacks a direct explanation in terms of folding models and can be viewed as an extension of the original concept of an OMP.

Undulations found in certain precision fits to elastic scattering data resemble those arising as a result of coupling to reaction channels [2]. Such undulations also occur in the l-independent potential found by inversion of the elastic channel S-matrix from coupled channel (CC), coupled reaction channel (CRC) or continuum discretized coupled channel calculations (CDCC). Furthermore, such

undulations also occur in the l-independent S-matrix equivalents of explicitly l-dependent nucleon-nucleus or nucleus-nucleus that fit elastic scattering data [2]. Thus, an extension of the OMP to include l dependence makes it possible to exploit precision data in a way that links it to the dynamics of elastic scattering.

Terminology used. In what follows, CC often indicates coupled channels in general, including CRC as well as CDCC for coupling to breakup channels. In the literature, "l-dependent" has sometimes been used to describe potentials that are parity-dependent, parity dependence being a particular form of l dependence in which the potential takes the form $V_{\rm W}(r) + (-1)^l V_{\rm M}(r)$ where the W and M subscripts label the (complex) Wigner and Majorana components. This work is a review of nuclear l dependence, referring to any dependence of the nuclear OMP on the partial wave angular momentum l, including parity dependence.

We refer to potentials having the same S-matrix, S_{lj} (and thereby the same values of all observables), as "S-matrix equivalent". Every l-dependent potential has an l-independent S-matrix equivalent that can be found by inversion.

Outline. Section 2 explains why, on the basis of standard theories, the OMP might be expected to depend on angular momentum. Much of the discussion is based on light-ion, mostly nucleon, scattering. The nucleon OMP has particular significance as a continuation into positive energies of the shell model single-particle potential. Section 3 addresses the particular case of parity dependence. Section 4 is a brief account of S-matrix inversion, defining certain frequently used terms. Section 5 discusses the extent to which l dependence can be linked to experiment. Section 6 surveys cases in which the contribution to the OMP due to channel coupling has been determined, with results that, it is argued, imply dynamically induced l dependence for (mostly) nucleons and loosely bound nuclei. Section 7 links the two previous sections, relating undularity found by fitting data to the undularity of calculated DPPs. Section 8 presents examples from the scattering of heavier nuclei, connecting l dependence to theory and experiment; angular momentum dependence is a general property of nucleus-nucleus interactions. Section 9 discusses what the existence of l dependence implies for phenomenological applications of OMPs. It also states the requirement for demonstrating l-independence in particular cases. Section 10 presents a general review and conclusions.

2 l dependence and theories of the OMP

In the background to any discussion of l dependence are various theories of the OMP. Two well-developed theories are i) the theory due to Feshbach [11,12] and ii), theories going back to Bell and Squires [13], a theory based on the self-energy of a nucleon in nuclear matter. The latter has especially been developed by Mahaux and collaborators [14–16], see also [17–19]. As emphasized by Mahaux and Satchler [20] there are fundamental differences between these two approaches, not the least being that there is no self-energy theory for the scattering of composite nuclei (but see ref. [21]). Feshbach's approach has long given insight into the scattering potentials for composite systems but applications have generally been rather phenomenological and, although exchange processes have been considered formally [12], fully antisymmetrized applications are difficult to implement.

Other reaction theories such as the resonating group model, RGM, also contribute to our understanding of interactions between lighter composite nuclei, particularly with the exploitation of S-matrix-to-potential inversion. RGM and related theories [22–24] include antisymmetrization exactly, enabling them to reveal information concerning parity dependence, as well as more general forms of l dependence, that arise from antisymmetrization.

2.1 Feshbach theory

The theory of Feshbach [11] has occasionally been employed in calculations of the total contribution to the nucleon OMP of all the channels that are coupled to the elastic channel, see *e.g.* [25–27]. However, more commonly, a form of this theory underlies calculations of the contributions of specific selected channels to the OMP, for example in various cases where it is apparent that particular processes are not represented in conventional calculations [28–30]. It can represent processes that vary with nuclear properties in a way that is excluded from the smoothly varying OMP of standard folding models. Such varying contributions are identified as the "dynamic polarization potential", DPP, see *e.g.* [30]. In the formal Feshbach theory the OMP or DPP are explicitly l-dependent and non-local, as manifest in ref. [27]. Nevertheless, local and l-independent representations of the non-local and l-dependent DPP can be found by S-matrix inversion; for recent examples see refs. [31–36]; reference [34] is an erratum for ref. [32]. In general, local and l-independent potentials representing DPPs exhibit undulatory, "wavy", features. Such features can be compared with features of l-independent potentials that are S-matrix equivalent to explicitly l-dependent potentials having known l dependence. These connections will be reviewed at length in what follows.

Invariably, local equivalent DPPs that represent coupling to specific channels can *not* be represented as a uniform factor multiplying the "bare" potential without the coupling. In many cases, DPPs can be reliably determined far into the overlap region of the interacting nuclei and, for nucleon scattering, over the whole radial range. These facts have consequences for the evaluaition of all OM theories since uniform renormalization cannot represent the contribution of channel coupling.

Although the many contributions to the full Feshbach OMP might somehow average to an effectively l-independent potential, specific contributions to strongly coupled channels vary with the target nucleus and depend upon the l transfer, Q-values, etc. It is implausible that these do *not* lead to l dependence and implausible

that such l dependence can be represented as a local form varying smoothly over a range of nuclei and energies.

2.2 Potentials derived from self-energy

Nucleon-nucleus potentials due to Mahaux and collaborators [14–16] and their later extensions, refs. [37,38], known as "JLM potentials", provide a satisfactory, but not precise, fit to nucleon elastic scattering data over a wide range of energies and target nuclei. The formalism [14–16] itself includes a local equivalent to the specific non-locality that arises from knock-on exchange, the major source of energy dependence of the JLM potentials. For a given energy, the JLM complex potential $V(r)$ depends on just the proton and neutron densities at radius r: the local density approximation LDA. The original local density model of refs. [14–16] was modified (the "extended local density approximation" of refs. [37,38]) in order to correct in a phenomenological way the radial extension of the potential. When applied, this model requires overall normalization factors to optimize fits to data.

Although the local density approximation was "extended" [14–16] to correct the radial size of the potential, it is still a local density model, based only on the nucleon densities of the nucleus, and not, for example, the density gradient. Specific properties of the nucleus such as its collectivity do not enter and nothing in the model corresponds to the orbital angular momentum of the interacting nucleon. Fits to data do not in general, approach $\chi^2/F = 1$, even with uniform normalization factors which cannot accurately represent channel coupling. The model leaves room for l-dependent terms.

2.3 Nuclear structure approach

The Nuclear Structure Approach of Vinh Mau [39] and others [40–43] incorporates some of the physics of the Feshbach approach with the self-energy method. In particular, it includes the effect of coupling to particle-hole states corresponding to giant resonances, and the relationship of this coupling to l dependence will be mentioned later. The effect of such resonances has been incorporated into optical model studies by Pignanelli *et al.* [44] and Delaroche *et al.* [45], and see also [46]. The calculations of ref. [43] are of particular interest since they recognize the generation of l-dependence within the model, and we shall refer to them again below. These calculations involve much the same physics as the calculations of Rawitscher [27] mentioned above.

We mention here that the optical model is discussed in the important monograph of Mahaux and Weidenmüller [47] who make explicit an approximation of their model which appears to be implicit in calculations based on the nuclear structure approach. This assumption is that there is just one nucleon in the continuum. This would exclude a contribution from processes such as the coupling to deuteron channels. The contribution of coupling to pickup channels can be, and has been, studied within an extended Feshbach model [26], as discussed below.

2.4 Limits of local density models

Nothing in models based on the local density approximation corresponds to l, the orbital angular momentum of the nucleon. There is no scope for the l of a scattering nucleon to influence a nuclear interaction within models in which the finite size of the nucleus and the density gradients in the nuclear surface enter only through the way that the interaction at radius r depends on the density around r. However, the excitation of inelastic channels involves projectiles in coupled channels propagating in potential gradients around the nucleus. The coupling leads to non-locality and l dependence that are not represented within the LDA. In Austern's picture of non-locality [48], flux leaves from the elastic channel at one location and is restored at another location. This second location will in general have a different local density. In the temporal non-locality discussed by Mahaux and Satchler [20], one can assume that the projectile will return to the elastic channel after it has propagated to a region of different density. The non-locality and l dependence that are due to collective channel coupling will have effects on direct reactions, and these effects have been studied in ref. [49].

The density gradient in the nuclear surface plausibly leads to l dependence. Consider an incident nucleon interacting with a target nucleon in the surface, where there is a nuclear density gradient. The reaction back on the incident nucleon depends upon whether the target nucleon recoils into an increasing or a decreasing nuclear density. This suggests a new term in the potential proportional to $\mathbf{k} \cdot \nabla\rho(\mathbf{r})$, *i.e.* for a spherical nucleus,

$$V_{\rm k}(r) = \mathbf{k} \cdot \mathbf{r} \frac{\partial\rho(r)}{\partial r} \,. \tag{1}$$

Here $\hbar\mathbf{k}$ is the local nucleon momentum. At high enough energies, where the eikonal approximation is good, $\hbar\mathbf{k}$ may be taken as the incident momentum, in which case a $\mathbf{k} \cdot \nabla\rho(\mathbf{r})$ will make a zero contribution, as can be seen from the eikonal integral for interaction $f(r)\mathbf{k} \cdot \mathbf{r}$:

$$\chi(b) = -\frac{1}{\hbar v} \int_{-\infty}^{\infty} f(r)\mathbf{k} \cdot \mathbf{r} \mathrm{d}z, \tag{2}$$

identifying kb with $l + \frac{1}{2}$ and $S(b) = \exp(\imath\chi(b))$ as usual. However, the relationship to l dependence is immediately apparent with the help of Pythagoras,

$$l^2 = k^2 r^2 - (\mathbf{k} \cdot \mathbf{r})^2 \tag{3}$$

which holds when $\hbar k$ is the local momentum. This implies that

$$\mathbf{k} \cdot \mathbf{r} = \pm\sqrt{k^2 r^2 - l^2}, \tag{4}$$

where the plus and minus signs apply at the outgoing and incident sides of the target nucleus. These effects would

not cancel where the projectile is substantially absorbed or where the eikonal approximation fails. If such a term were effective, it would constitute a source of l dependence. The formulation would be more elaborate if a self-consistently calculated complex local momentum were to be included in a term of the form $\mathbf{k} \cdot \nabla\rho(\mathbf{r})$.

2.5 Implications of channel coupling

A long history of calculations reveals that coupled channels, including reaction channels, make a substantial contribution to elastic scattering. The contribution of low lying vibrational states to the proton OMP was studied by Buck [50] and Perey [51], and the contribution of rotational excitations of deformed nuclei, to the OMP for other projectiles, was studied in refs. [28,29]. For proton scattering, it was found [52,53] that coupling to deuteron channels by neutron pickup substantially modified the calculated observables, in one case [54] greatly improving the fit for 30.3 MeV protons on ^{40}Ca, a notoriously hard case to fit (cf. sect. 7.5); the deep minimum in the angular distribution around 140° was fitted. Later calculations, in which various approximations were lifted, reduced the effect, although the recent studies [32,34,55,35] of this case still reveal a substantial DPP arising from the coupling to deuteron channels. Although the deep minimum in the angular distribution near 140° is no longer fitted, the coupling does have a large effect on the whole of the angular distribution. The radial form of the DPP is very far from a uniform renormalization of the "bare" (folding model) potential: the real part is attractive close to the nuclear center, with a repulsive region further out. The imaginary part is absorptive towards the nuclear center becoming almost emissive in the nuclear surface; the real and imaginary spin-orbit terms of the DPP are more undulatory ("wavier") than the central terms. Such undularity is characteristic of potentials that are l-independent representations of l dependent potentials (*i.e.* having identical S-matrices), as is discussed in sect. 5.3.

As mentioned in sect. 2.3, refs. [44,45] studied the effect on proton elastic scattering of coupling to high-lying giant resonances. This coupling led to quite a good fit to the backward angle minimum for scattering from ^{40}Ca [44] and also from ^{16}O [45]; such coupling appears to be necessary together with coupling to pickup channels. The contribution of the giant resonances must be present for all target nuclei, not just closed shell nuclei ^{16}O and ^{40}Ca. For these nuclei the effect becomes apparent because there exist deep minima in the elastic scattering angular distributions which are not filled in by the many active processes that apply for nuclei away from closed shells. The systematic contribution of giant resonance coupling to l dependence is not yet known. This contribution to the OMP is likely to vary with energy and target nucleus in a different way to the contributions of low-lying collective states and particle transfer. A recent study of the DPP for protons coupled to both low lying and high lying collective states, is ref. [36]; the equivalent local potentials are very undulatory, indicating l dependence.

A more complete listing of DPP calculations leading to undulatory DPPs for nucleon scattering is given in sect. 6.2.

2.6 Relating coupled channel effects to l dependence

Reference [56] compared the contribution to the elastic scattering S-matrix, S_{lj}, that is due to coupled neutron pickup channels, ref. [54], with the contribution to S_{lj} of a phenomenological l-dependent term. This comparison indicated that at least part of the l dependence is due to pickup channel coupling.

Subsequently, coupled reaction channel (CRC) calculations became much more highly developed enabling much more rigorous comparisons of the same kind involving explicitly l-dependent potentials fitted to data. S-matrix-to-potential inversion, see sect. 4, makes it possible to invert S_{lj}, for any given l-dependent potential to give the l-independent equivalent. In the same way, the elastic channel S_{lj} from any CC calculation can also be inverted to give the corresponding potential. The resulting l-independent potentials can be compared making it possible to match empirical l dependence with l dependence arising from channel coupling.

Delaroche *et al.* [45] examined the effect of coupling to giant resonances upon $|S_{lj}|$ but not upon $\arg(S_{lj})$. As shown in [56], it is the argument of the S-matrix which relates most directly to the effect on the real part of the potential, especially for nucleons. The combination of l transfer and momentum transfer involved in exciting giant resonance states is a likely source of l dependence, and this deserves exploration.

Franey and Ellis [57] calculated a "trivially equivalent local potential", TELP, from the elastic channel partial wave functions of a CC calculation. In this way, there was an individual potential for each partial wave l. Such potentials make explicit the l dependence due to channel coupling, but the irregular dependence on l has led to little effort to interpret them. However, l-weighted TELPS are approximate l-independent representations of the DPP, and code for this is incorporated in the FRESCO CC code [58]. For remarks on the validity of weighted TELPS, see sect. 6.3.

Section 6 discusses l dependence due to channel coupling at length.

2.7 The contribution of knock-on exchange

It is generally believed that knock-on exchange, represented by the Fock term in the interaction between a scattered nucleon and the bound nucleons, is responsible for most of the energy dependence in the effective local nucleon-nucleus interaction, the nucleon OMP. The contribution of knock-on exchange is included as a local approximation in standard folding models, *e.g.* refs. [14–19,37,38]. The explicit inclusion of knock-on exchange requires the solution of integro-differential equations, *e.g.* refs. [59–62], and is seldom carried out. The phenomenological non-local

potential of Perey and Buck (PB), ref. [63], accounts for the energy dependence of the local nucleon OMP, as shown explicitly in ref. [64] in which S_{lj} for the PB non-local potential was inverted to produce the local equivalent. The inverted potential in this case did not appear to be l-dependent suggesting that knock-on exchange does not lead to l dependence. However, Lukaszek and Rawitscher, ref. [65], have shown that a realistic non-local exchange term, derived from a non-local nuclear density, does give rise to l dependence in the nucleon-nucleus local interaction. This l dependence does not appear to be parity dependence and deserves further study. The calculations of ref. [65] apparently reveal a limitation of the symmetrical form of non-locality of Perey and Buck. Nuclear matter calculations show that, in a *uniform* medium, exchange non-locality does indeed [66] have the Gaussian form of Perey and Buck; however it is just the existence of a nuclear surface that opens the possibility of l dependence, see also ref. [43] mentioned in sect. 2.3.

2.8 l dependence and causality

Causality imposes a relationship between the energy dependencies of the real and imaginary components of the OMP, see *e.g.* [67]. This must imply a relationship between the l dependence of the real component and the l dependence of the imaginary component. This means that for each value of the conserved quantity l there is a dispersion relation linking the two components [68]. The consequences of this have not been consistently pursued, but they have been studied in one case as reported in sect. 8.2. More generally, it seems inevitable that l dependence in either the real or imaginary term will be accompanied by l dependence in the other term.

3 The special case of parity-dependence

Particular exchange processes, especially important for scattering between light nuclei, give rise to parity dependence leading to corresponding exchange terms in the potential. Historically, such parity dependence has been represented phenomenologically by the inclusion of a term in the real part of the OMP that depends upon the partial wave angular momentum l:

$$V(r)(1+\alpha(-1)^l) \tag{5}$$

with a similar term for the imaginary potential. We refer to specific cases below. Equation (5) is not the most general form of parity dependence, a more general expression involving four independent radial terms, for the real and imaginary Wigner and Majorana components,

$$V_{\rm W}(r)+(-1)^l V_{\rm M}(r)+{\rm i}(W_{\rm W}(r)+(-1)^l W_{\rm M}(r)). \tag{6}$$

Such parity dependence is generated by almost all exchange terms arising from antisymmetry, with the exception of knock-on exchange of sect. 2.7 (but see ref. [65]).

An exchange term that does induce parity dependence is heavy particle stripping. An example of this would be the contribution to the elastic scattering of a proton on ^{16}O when the incident proton picks up ^{15}N, leaving a proton. Exchange terms are always present due to the antisymmetrization of projectile and target nucleons, such as explicitly represented in resonating group model, RGM, calculations.

Parity dependence has been studied phenomenologically by fitting data, see sect. 3.2 below and sect. 7.4; strong parity dependence was revealed in some cases. Such fits to data have usually involved parity dependence of the less general kind, eq. (5).

3.1 Parity dependence linked to theory

Support for parity dependence leading to Wigner and Majorana components, eq. (6), comes by inverting S_{lj} from resonating group model, RGM, calculations (S-matrix to potential inversion is discussed in sect. 4). This has been done for proton scattering from nuclei from mass 4 to mass 40, as reviewed in [69] and discussed below. Baye [70] has presented theoretical arguments for the way in which the strength of parity dependence is related to the masses of two interacting nuclei. If one of these is a nucleon, then the Majorana terms become smaller as the mass of the target nucleus increases. These predictions are borne out by studies of two complementary kinds (see ref. [69]): i) S-matrix to potential inversion of S_{lj} found by R-matrix and other fits to scattering data, and ii) S-matrix to potential inversion of S_{lj} from RGM calculations. For nucleon scattering from ^{4}He, the same general result follows from studies of both type i) (data fitting) and type ii) (RGM): that is, the odd-parity real potential has both volume integral and RMS radius substantially greater than the even-parity potential. This is inconsistent with the form of eq. (5).

Reference [69] reports parity dependence in many other cases of nucleus-nucleus scattering. As Baye predicted, the strength of the Majorana term for proton scattering falls off with the mass of the target nucleus, but is still substantial for nucleon scattering from ^{16}O, as found also in ref. [71] although that work was based on imperfect fits to data. We return to parity dependence of nucleons on ^{16}O in sect. 7.4 where strong evidence for it together with evidence for coupling-induced l dependence is discussed. None of the parity dependent potentials from studies of type i) or type ii) have an overall factor $(1+\alpha(-1)^l)$, the standard assumption of purely phenomenological fits to experimental elastic scattering data, see sect. 3.2 below.

In nucleon scattering from ^{6}He, the parity dependence is, as expected [70], less than for nucleon scattering from ^{4}He, but still substantial, see ref. [72]. An extreme case of parity dependence, as determined from RGM S-matrix elements, is for ^{3}He on ^{4}He, see ref. [73]. This reference also presents parity-dependent potentials for ^{3}H on ^{4}He inverted from RGM-derived S-matrix elements. Reference [74] presents RGM-derived potentials for nucleons scattering from light target nuclei that have non-zero spin; in such cases the character of the parity dependence

strongly depends upon the channel spin. References [69, 75] review further cases where parity dependence has been well established from RGM S-matrices which include exchange effects explicitly.

3.2 Parity dependence supported by fits to data

Parity dependence leads to the enhancement of differential cross sections at backward angles. This is often due to heavy particle stripping in the case of nucleon scattering or cluster transfer in interactions between heavier nuclei. One example of the latter is alpha particle transfer in the case of ^{16}O scattering from ^{20}Ne. For alpha particle scattering from ^{20}Ne, Michel and Reidemeister [76] showed that a small Majorana term markedly improved the fit to elastic scattering angular distributions, apparently due to knock-on exchange of an α cluster. A problem occurs in establishing parity dependence: S_l that originates from the parity-dependent potential can always be fitted, by $S_l \rightarrow V(r)$ inversion [69], with an l-independent potential. In the α plus ^{20}Ne case, and in spite of the smallness of the Majorana term, the l-independent potential was found [77] to be markedly undulatory. Such undularity would not have been discovered by fitting the elastic scattering angular distributions in the usual way.

The enhanced backward angle differential cross-section, that is characteristic of exchange processes, occurs in the elastic scattering of ^{12}C on ^{16}O. This backward angle enhancement has been explicitly shown [78] to be due to α exchange. More recently, this backward angle effect has also been shown [79] to be representable within a potential model by the inclusion of real and imaginary Majorana terms. For further concerning this case, see sect. 8.3.

The generation of parity dependence by exchange processes was recognized in phenomenological analyses: calculations for $n+\alpha$ scattering [80] included a Majorana term in the real potential. Subsequently, an imaginary Majorana term was included in an analysis of $p+\alpha$ scattering [81]. These studies involving light target nuclei suggested the application to heavier nuclei, and real and imaginary Majorana terms were included [82] in an analysis of proton scattering from ^{40}Ca. This work showed that small parity-dependent terms had a large effect at far backward angles but it was not conclusive since other effects are clearly important in this case, as discussed in sect. 7.5 below. However, this work did inspire a more extensive exploration [71] of the possible need for Majorana terms in the general nucleon OMP. Reference [71] found that Majorana terms were important for $p+{}^{16}$O, less so for a ^{40}Ca target and negligible for scattering from heavier nuclei.

Parity dependence has been firmly established by fitting experimental data for nucleon scattering from ^{4}He [83] and ^{16}O [84] and for ^{3}He scattering from ^{4}He, see ref. [85]. The parity dependence of the interaction for ^{4}He scattering from ^{12}C [86] has been established by inverting S_l precisely fitted to data over a range of energies. A potential applicable at the lowest energies was determined. The volume integral $J_{\rm R}$ (as defined in ref. [30]) for odd parity was $\sim 425\,\mathrm{MeV\,fm^3}$ whereas that for even parity was $\sim 390\,\mathrm{MeV\,fm^3}$. This difference might be significant for tunneling at astrophysical energies where $l=0$ dominates; in that context a parity-independent potential fitted to data for this system would be misleading since it would be influenced by the need to fit the odd-parity S_l.

3.3 Parity dependence —general considerations

Although the origin of parity dependence makes it somewhat distinct from other forms of l dependence, the problem of understanding its l-independent representation is part of the same formal problem as the l-independent representation of dynamical l dependence. Reference [31] presents the l-independent equivalent for an l-dependent potential, the real part of which had a factor $(1.0 + 0.05(-1)^l)$, for 15.66 MeV protons incident on ^{8}He. The imaginary part as well as the real part of the equivalent potential had undulations, including a small excursion into emissivity in the imaginary part.

Model calculations [87], in which S_l for explicitly parity-dependent potentials were inverted, led to oscillatory l-independent potentials. The volume integrals of the oscillatory potential were virtually the same as for those including a Majorana factor. It was stated: "The fact that a large Majorana term makes little difference to the volume integral of the equivalent l-independent potentials undermines the logic of the common argument to the effect that the agreement between $J_{\rm R}$ and $J_{\rm I}$ for global optical optical potentials and nuclear matter theory indicates that the essential features of the optical model are well understood." See also ref. [88].

Parity dependence is not the only form of l dependence that results from antisymmetrization, see sect. 8.1 for examples arising in interactions of mass-16 nuclei.

4 S-matrix to potential inversion

This review frequently considers potentials that give rise to particular elastic scattering S-matrices, S_l, or S_{lj} for spin half projectiles (spin 1 projectiles involving a non-diagonal S-matrix can be handled but that case is not discussed here.) While it is simple to derive S from potential V (the direct problem), the inverse problem is less simple. Early studies of S-matrix inversion are in refs. [89,87,90]; for more recent reviews see refs. [69,75, 91,92]. All the inversions reported herein employed the iterative-perturbative, IP, inversion method [89,87,90,69, 75,91,92].

In what follows, the S-matrices have been inverted using the iterative-perturbative, IP, $S_{lj} \rightarrow V(r)+\mathbf{l}\cdot\mathbf{s}\,V_{\rm SO}(r)$ inversion algorithm which is presented in refs. [93,91,75, 94]. The IP inversion is implemented in the inversion code IMAGO [95] which quantifies the difference between the S^t_{lj} to be inverted and the S^i_{lj} of the inverted potential in terms of the S-matrix distance σ defined as

$$\sigma^2 = \sum_{lj} |S^t_{lj} - S^i_{lj}|^2. \qquad (7)$$

The IP iterations start from a "starting reference potential", SRP. When inversion is applied to the elastic channel S-matrix from a coupled channel calculation to determine the DPP due to the coupling, the SRP will be the bare potential of the coupled channel calculation. Where inversion is applied to determine the l-independent equivalent of an explicitly l-dependent potential, generally a potential with an l-dependent term added to an l-independent potential, the SRP will generally be the l-independent component.

The plots of the inverted potentials presented in this review generally include the SRP. In such plots, the contribution of the channel coupling (or the l-dependent term) to the inverted l-independent potential thus appears as the *difference* between the inverted potential and the SRP. In the case of channel coupling, these differences of the various components together represent the DPP; in the case of inversion of S_{lj} from a potential containing an explicit l-dependent term, these differences together are an l-independent representation of the l dependence.

The IP method can yield inverted potentials that are effectively independent of the SRP. The uniqueness of the inverted potential can be tested by the use of alternative "inversion bases", see refs. [75,94]. The IMAGO program provides the values of σ and in cases where two inverted potentials are shown, that with the lower σ is generally adopted. The tendency for undularity to increase as σ becomes very small will be addressed in relation to the significance of the potential undulations.

In this review, two potentials, one of which may be l-dependent, that lead to the same S_l or S_{lj}, are said to be "S-matrix equivalent." Clearly, they lead to identical observables.

The inverted local and l-independent DPPs arising from channel coupling will be shown to exhibit undulatory (wavy) features of a kind that cannot arise from any undulatory features in nuclear densities. Such features are characteristic of potentials that are S-matrix equivalent to explicitly l-dependent potentials.

5 Experimental evidence for l dependence

5.1 The problem of identifying l dependence

There is a particular difficulty in establishing l dependence convincingly since any S-matrix S_l, depending on partial wave angular momentum l, can be subject to $S_l \rightarrow V(r)$ inversion [69,75,91,92] (or $S_{lj} \rightarrow V(r) + \mathbf{l} \cdot \mathbf{s}\, V_{\rm SO}(r)$ inversion; the possibility of spin-orbit inversion is implicit when not stated) leading to an l-independent potential. For example S_l for an explicitly parity-dependent potential can be inverted to yield a parity-independent potential. Any l-independent potential that is S-matrix equivalent to an l-dependent potential will be undulatory, ranging from mildly wavy to markedly oscillatory, as examples will show.

Two S-matrix equivalent potentials (l-dependent and l-independent) yielding the same S_{lj} will, in general, lead to different wave functions within the range of the potential. In many contexts an l-dependent potential is arguably more physical than a very undulatory l-independent equivalent. Any elastic scattering data can be fitted by a local l-independent potential, perhaps determined by model-independent fitting (sums of spline functions, Bessel functions etc.) or by fitting S_{lj} to the data followed by inversion of S_{lj}. In either case, finding an undulatory potential probably indicates an underlying l-dependent potential.

Although it is easy to find an l-independent equivalent to any given l-dependent potential, the inverse to this, *i.e.*, identifying the specific form of l dependence from empirical waviness, is an open problem. It is always possible to find complex coefficients $f(l)$ for any $V(r)$ such that, for all l, $f(l)V(r)$ reproduces given S_l, but this will not be easily interpreted.

The many possible forms of l dependence make establishing unique l dependence by fitting experimental data with such forms a daunting task. In principle, model independent fitting should achieve a perfect ($\chi^2/{\rm DF} \sim 1$) fit to observables that have been measured with high precision over a wide angular range. Such precise fits should provide uncertainties and may yield wavy potentials (for 52 MeV deuterons, see ref. [96], for 20 MeV deuterons see ref. [97], for protons, see refs. [98,99]) and "all" that remains is to establish a correspondence between the particular undularity found by the search and the corresponding forms of l dependence.

Establishing l dependence, as a signature of the limitations of the local density approach, is of sufficient interest that the extraction of the full information content of elastic scattering data, by precisely fitting that data, is a worthwhile objective. In fact, attempts to extract the full information content of the data have become rare. Claims for the "limitation of the one-channel phenomenological optical model" [100], based on the failure to achieve fits with (visual estimate) $\chi^2/N \sim 20$, are clearly invalid. A failure of Woods-Saxon, WS, potentials to achieve $\chi^2/N \sim 20$, or even $\chi^2/N \sim 1$, is *not* a failure of the phenomenological optical model, but the failure of an unnecessarily restricted form of potential. It is always possible to find a complex potential giving a perfect fit; the problem is one of interpretation. The problem is also an opportunity.

The belief that it is worthwhile to extract the full information content from hard-won, high precision elastic scattering data, is less universal than the commonly expressed belief that a fit with $\chi^2/N \sim 20$ is "good". What constitutes a "good fit" can be a matter of context, but contexts certainly exist where it is appropriate to extract the full information content of the data. How to do this is unclear since there will always be an l-independent equivalent to any l-dependent potential that precisely fits the data; it will certainly not be of Woods-Saxon form. In fact, there may be many potentials giving perfect fits, when, for proton scattering, there is no measurement of the Wolfenstein spin-rotation R-parameter, see ref. [101]. Little is known of the topology of the region in parameter space defined by $\chi^2/{\rm N} \sim 1$, for data of specific quality, see ref. [102]. Thus, such properties of the nucleon-nucleus interaction

as its possible l dependence can be hard to establish unambiguously, even from precise fits for a single nucleus at a single energy: such fits are necessary but not sufficient. In this connection note that model-independent fits to proton scattering, presented in ref. [99], did not achieve a precise fit to 30.3 MeV proton scattering from ^{40}Ca, missing exactly the feature at backward angles that motivated the original l-dependent fits. It appears that very close fits were not sought just because of the emerging undulations.

Another model-independent fit for the same case, ref. [98], applying "theoretically unprejudiced fits" actually was at fault because the following prejudice was applied in the search: the imaginary potential was constrained to be nowhere emissive. It is now known that this is not required for maintaining the unitarity limit, and it is commonplace for DPPs generated by channel coupling to have emissive regions without breaking the unitarity limit. Explicitly l-dependent potentials commonly have l-independent equivalents with emissive regions, as shall be seen in examples given below.

Finally, we stress that most elastic scattering data is *incomplete*, and not just because of the lack of spin-rotation measurements, of which there are almost none for proton elastic scattering. For protons there are very commonly no measured angular distributions or analysing powers for significant parts of the angular range. The situation for neutrons is worse. This is often an unavoidable consequence of experimental circumstances, but the consequences of this incompleteness should be recognized. The way in which the restricted angular range bears directly on the question of l dependence for the case of ^{3}He scattering, is explained in sect. 5.4.

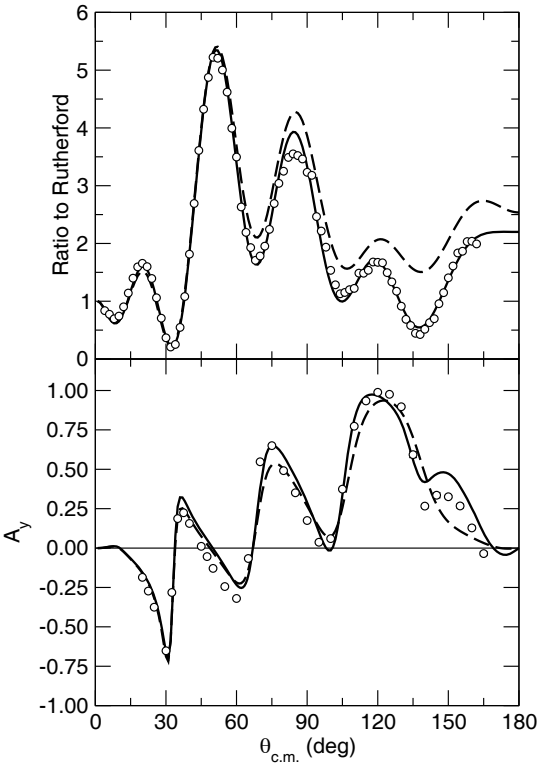

Fig. 1. For 30.3 MeV protons on ^{40}Ca, the solid lines are the angular distribution (above) and analyzing power for the l-dependent potential of ref. [103]. The dashed lines are calculated with the same potentials except that the l-dependent component is omitted; the difference represents the effect of the l-dependent component.

5.2 Direct evidence for l dependence from fits to nucleon elastic scattering

In ref. [103] an l-dependent term was added to an OMP of standard form leading to a substantial improvement to fit to the angular distribution and analyzing power data for 30.3 MeV protons scattering from ^{40}Ca. The data were of unusual precision and of wide angular range and had resisted all attempts to achieve low χ^2/N. The l-dependent term, which was added to a standard 7-parameter WS plus WS-derivative l-independent central potential, had the following l^2-dependent form:

$$U_l(r) = f(l^2, L^2, \Delta^2)(\tilde{V} g_{\rm R}(r) + {\rm i}\tilde{W} g_{\rm I}(r)) \qquad (8)$$

where the functions $g_{\rm R}(r)$ and $g_{\rm I}(r)$ are standard WS derivative terms and $f(l^2, L^2, \Delta^2)$ is the standard WS form with L^2 being the "radius" and Δ^2 the "diffusivity". The spin-orbit component had no l-dependent term. The l-dependent potential did fit the deep minimum in the angular distribution around 140° that no WS (or folding model) potential has fitted. Reference [103] compared the best fits to the data by the l-dependent potential and the best WS l-independent potential, fig. 1 of that reference comparing the angular distributions and fig. 2 comparing the analysing powers. Here, fig. 1 shows the contribution of the l-dependent term within the overall l-dependent potential of ref. [103]. To do this we compare the angular distribution and analyzing power due to just the l-independent part of the l-dependent potential (dashed line) with the same quantities calculated with the full l-dependent potential (solid line). The substantial change in both quantities includes the appearance of a conspicuous minimum near 140°. For the fit to the angular distribution, the reduction in χ^2_σ/N_σ is from 34 to 4.88. The reduction for the analysing power, χ^2_a/N_a is more modest.

The l-dependent added term, eq. (8) introduced in ref. [103], was applied in fitting angular distribution and analysing power data for the elastic scattering of nucleons on ^{16}O, ^{40}Ca, ^{56}Fe and ^{58}Ni over a wide range of energies in ref. [104]. It was later applied to further nuclei from ^{15}N to ^{208}Pb in ref. [105]. Much better fits, with much lower χ^2/N than possible with standard Woods Saxon (WS) potentials, were found over a wide range of energies. Both the parameters and the properties, such as volume integrals and rms radii of the l-independent component, behaved in a more regular fashion than the same properties of the best standard l-independent WS fits. The only exceptions to this regularity were suggestive resonance-like features appeared at certain energies on otherwise smoothly varying volume integrals and rms radii. The same quantities for the corresponding best l-independent WS fits were more

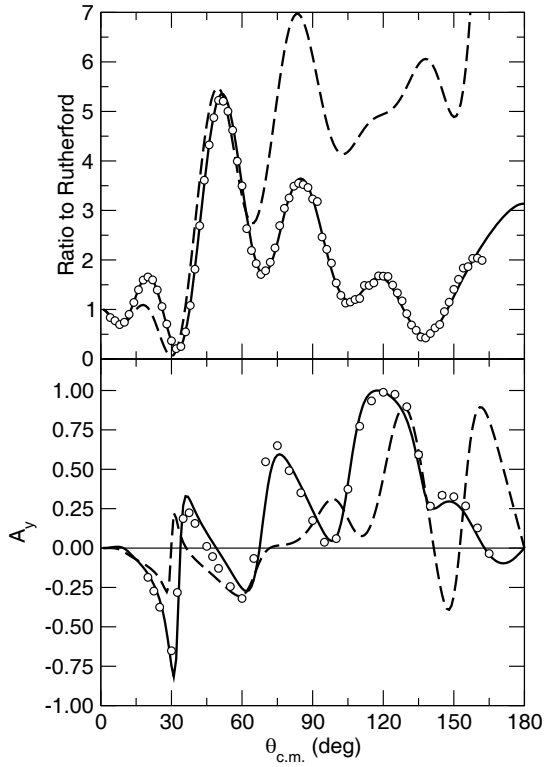

Fig. 2. For 30.3 MeV protons on ^{40}Ca, the solid lines are the angular distribution (above) and analyzing power for the l-dependent potential of ref. [104]. The dashed lines are calculated with the same potentials except that the l-dependent component is omitted; the difference represents the effect of the l-dependent component.

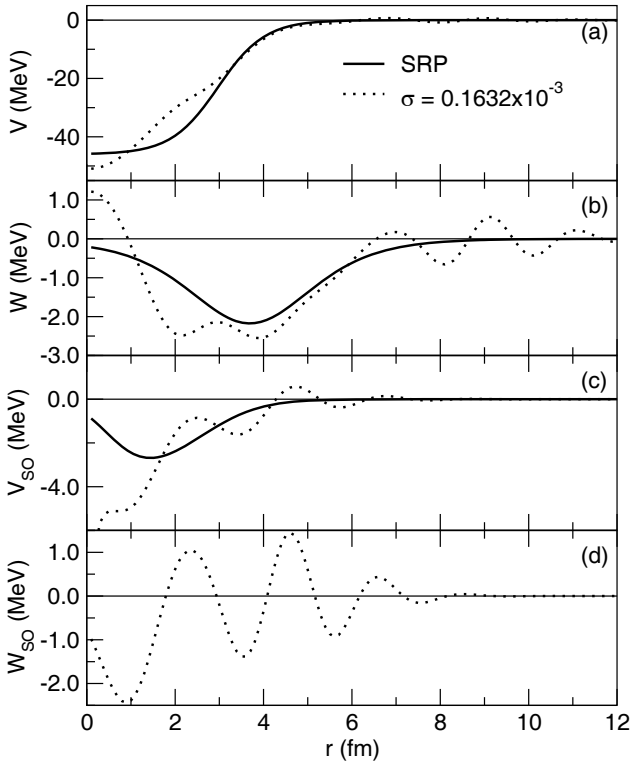

Fig. 3. For 30.1 MeV protons on ^{16}O, the solid lines present the l-independent part of the l-dependent potential ref. [104] and the dotted lines present the l-independent potential found by inversion. The difference represents the effect of the l-dependent component. The solid lines also represent the SRP for the inversion. From the top downwards, the panels represent the real central, imaginary central, real spin-orbit and imaginary spin-orbit terms. The σ value for the dotted line represents the S-matrix distance of the inversion defined in eq. (7).

irregular. Reference [104], in which the contribution of the l-dependent terms was very large, see fig. 2, presents better fits for 30.3 MeV protons on ^{40}Ca than ref. [103]. In this figure, the dashed curves are calculated with just the l-independent part of the l-dependent potential. The larger effect evident in fig. 2 is a consequence of the fact that the l-independent term of ref. [104] was, for 30.3 MeV, rather different from that of the earlier single-energy fit of ref. [103].

The conspicuously larger contribution of the l-dependent term in fig. 2 is related to both lower χ^2 and is also consistent with fits covering a wide energy range and several target nuclei. The general character of the l-dependence is the same for all energies and target nuclei. For the case of fig. 2, 30.3 MeV protons on ^{40}Ca, the fit corresponds to a reduction in χ^2_σ/N_σ from 20.25 to 2.09, where 20.25 is for the best l-independent potential. The reduction for the analysing power, χ^2_a/N_a, was from 20.48 to 13.74; there was no l-dependence in the spin-orbit term. The best-fitting l-independent potential was not the l-independent part of the l-dependent potential shown as dashed lines in fig. 2. For ^{40}Ca, comparable reductions in χ^2 per datum were achieved for 11 energies between 17.3 MeV and 48.0 MeV. Similar results were obtained for elastic scattering of protons from ^{16}O from 23.4 MeV to 52.5 MeV, and a few cases for ^{56}Fe and ^{58}Ni. In summary: substantial l-dependent contributions like that for 30.3 MeV protons on ^{40}Ca were part of a consistent pattern applying for a range of target nuclei and energies; subsequently, consistent results were found for a range of nuclei from ^{15}N to ^{208}Pb, see ref. [105].

5.3 Undularity as a consequence of l dependence

The relationship between l-dependence and the undularity (waviness) of the potentials that are S-matrix equivalent to explicitly l-dependent potentials is explored at some length in ref. [2]. Here we present some points of that discussion.

For protons scattering from ^{16}O at 30.1 MeV we present as dotted line in fig. 3 the potential which is S-matrix equivalent to the optimal l-dependent potential of ref. [104]. This is compared, solid line, with the l-independent potential to which an l-dependent term with the form of eq. (8) had been added.

For protons scattering from ^{40}Ca at 30.3 MeV we present as dotted and dashed lines in fig. 4 two inverted potentials, of successively lower inversion σ, representing

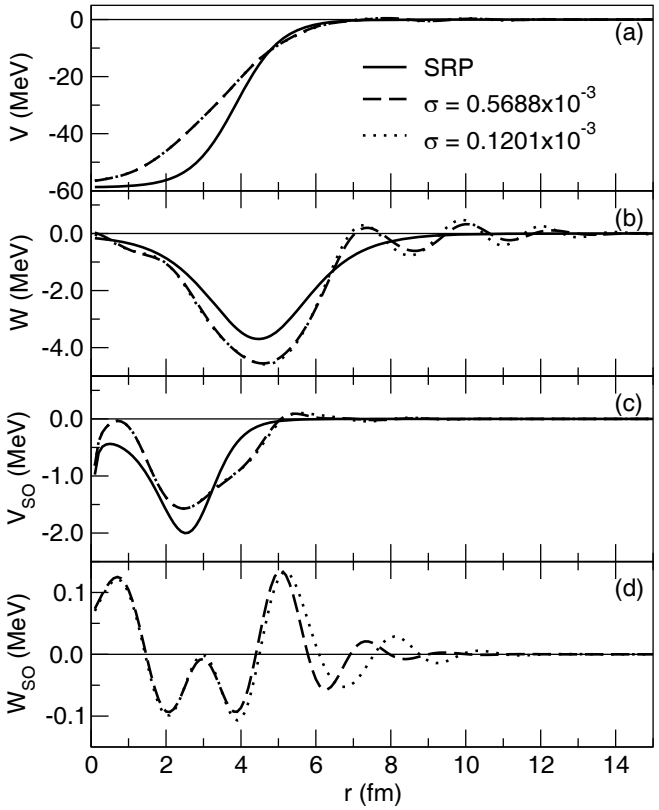

Fig. 4. For 30.3 MeV protons on ^{40}Ca, the solid lines present the l-independent part of the l-dependent potential ref. [104] and the dashed and dotted lines present l-independent potentials found by inversion. The dashed line with the larger inversion σ represents an earlier stage of the iterative inversion process. The differences between the dotted and solid lines represent an l-independent representation of the contribution of the l-dependent component. The solid lines also represent the SRP for the inversion. From the top downwards, the panels represent the real central, imaginary central, real spin-orbit and imaginary spin-orbit terms. The σ value for the dashed and dotted lines represent the S-matrix distance of the inversion defined in eq. (7).

the potential which is S-matrix equivalent to the optimal l-dependent potential of ref. [104]. These are compared with the l-independent potential, solid line, to which an l-dependent term with the form of eq. (8) had been added.

From fig. 3 and fig. 4 it will be evident that l-independent potentials that represent the ^{16}O and ^{40}Ca l-dependent potentials of ref. [104] at around 30 MeV, are highly undulatory. For larger radii, the undulations on the real and imaginary central terms are comparable, although the scale for the real part makes this unobvious. For other cases, see ref. [2]. Of particular significance are the excursions of the imaginary potentials into positive values. These are emissive regions but there is no breaking of the unitarity limit, *i.e.* $|S_{lj}| \leq 1$ for all l; this must be the case since the l-dependent potential did not break the unitarity limit.

The l dependence of ref. [104] and ref. [105], that fitted a wide range of elastic scattering nucleon data, had an l-dependent term that was of Woods-Saxon derivative form, peaked in the surface. The undularity of the l-independent equivalent did not depend on the surface nature of the l-dependent term. In sect. 8.3 it is shown that a simple l-dependent renormalization of a WS form leads to an l-independent potential with the key characteristcs: i) emissive regions, ii) undularity and iii) effects in the real l-independent potential that are due to imaginary l dependence, and *vice versa*.

The properties of the l-independent potentials, that are S-matrix equivalent to the l-dependent potentials fitted to proton scattering of refs. [104], are significant. For 30.3 MeV protons on ^{40}Ca, the undulations in both the real and imaginary central terms qualitatively resemble the undulations generated by coupling to vibrational states, as presented in ref. [36] and discussed below in sect. 6.2 and sect. 7.1. In particular, the imaginary central term has excursions into emissivity, ref. [106], that have magnitude and radius similar to those generated by coupling to vibrational states. Those emissive regions also do not lead to the breaking of the unitarity limit.

5.4 Evidence for l dependence in ^{3}He scattering

The angular distribution and analysing power for elastic scattering of ^{3}He at 33 MeV from ^{58}Ni could not be fitted by standard Woods-Saxon phenomenology. In particular, the fit to the angular distribution was poor from 120° to nearly 180°. In ref. [107], the same data were analysed with the same form of l dependence [103,104] that had been applied to proton scattering. The qualitative fit to the angular distributions was greatly improved for $\theta \geq 120°$ degrees with χ^2/N halved. Subsequently, the same l-dependent model was applied, ref. [108], to the scattering of polarised ^{3}He on ^{16}O and ^{40}Ca but in this case the l-dependent component did not improve the fit. The significant difference was that for both the ^{16}O and ^{40}Ca cases, unlike the ^{58}Ni angular distribution, the data terminated below 120°. This is a clear example of a case in which incompleteness of the data has concealed possible evidence for l dependence. It is a pity since ^{16}O and ^{40}Ca are, like ^{58}Ni, of low collectivity, leading to elastic scattering angular distributions with well-defined deep minima. Reference [109] presents elastic scattering angular distributions (ADs) for 33 MeV ^{3}He on Ni isotopes of varying collectivity. The backward angle fits for the least collective isotope, ^{58}Ni, with standard Woods-Saxon potentials, are much poorer than the fits for the more collective isotopes. We know this because of the relative completeness of the AD data for all these cases which extend to about 175°. This relationship between collectivity and ease of fitting applies to Ca isotopes. For nucleons scattering on calcium, it was the least collective isotope, ^{40}Ca, that revealed the requirement for l dependence in elastic scattering. It appears that, for nuclei with low-lying collective states, competing processes tend to wash out the sharp features in the angular distributions that make l dependence manifest.

5.5 Evidence for l dependence from singular behavior at the origin

The undularity of l-independent potentials representing l dependence was established in ref. [87] in which inversion of S_l for potentials with added l-dependent terms led to quite strong undulations. The waviness in the surface included regions in the surface where the overall attractive potential $V(r)$ was actually repulsive, but, significantly, $V(r)$ had a strong radial derivative at $r = 0$. As a consequence, the same potential in three dimensions, $V(\mathbf{r})$, would have a marked cusp at the nuclear center. Where a potential $V(r)$ is reliably established by phenomenology to have a non-zero derivative at $r = 0$, then the non-physical nature of a central cusp implies that the potential must represent an underlying l dependence. It is likely that most nucleon and deuteron elastic scattering analyses could have sufficient sensitivity to the $V(r)$ near $r = 0$ to establish a non-zero radial derivative in $V(r)$ there. The natural interpretation of such a property is that the potential is an l-independent representation of an l-dependent potential.

5.6 Evidence from S-matrix fitted to experiment

Inversion of S-matrices enables an alternative phenomenology: fit the elastic scattering data by direct searches on S_{lj} followed by inversion of the S_{lj}. In principle, χ^2/N of unity can be found. Moreover, error bounds could be placed on the S_{lj} which could then be propagated through to error bounds on the potential. The first step of this procedure was applied in ref. [101], the work in which the ambiguity that persists without measurements of Wolfenstein's spin-rotation parameter R was identified. However, even without R measurements, meaningful inversion of fitted S_{lj} can lead to interesting results.

In ref. [110] angular distributions and analysing powers of exceptional precision and angular range for proton elastic scattering from ^{16}O at 27.3 MeV and 34.1 MeV were studied. Searches on S_{lj} for all relevant l and j led to essentially exact fits to all that data. Inversion of these S_{lj} yielded real and imaginary, central and spin-orbit potentials, all of which exhibited undulatory features. The imaginary central terms had emissive regions and, most remarkably, in both cases strongly emissive features appeared at the nuclear centre. The real components had cusps at the nuclear centre. It was argued that the large degree of flux generation at the nuclear centre could not be a result of dynamical non-locality. There is no apparent alternative to l dependence. Arguably, further such studies involving direct fitting of the S-matrix are necessary. These should ideally include measurement of the spin-rotation parameter R which appears to be required to unambiguously determine a local potential that fits nucleon elastic scattering data. Such potentials, that exactly fitted the data, would be appropriate targets for theoretical calculations of the local nucleon-nucleus potential.

6 Inferring l dependence from channel coupling DPPs

The contribution of particular coupled channels to the phenomenological OMP is of interest since it relates OMPs to the specific properties of the target nucleus or the projectile. The nucleus-to-nucleus variation of collectivity and transfer reaction strength must affect the OMP in ways that are absent from standard folding models. This is why, for example, the helion global OMP of ref. [5] requires a "local" OMP near the ^{40}Ca closed shell.

DPPs that are deduced for specific channel couplings allow the identification of dynamical non-locality and l dependence with particular reaction processes. For general references concerning the DPP generated by channel coupling see sect. 2.1.

6.1 Determining DPPs by inversion

The general method of determining the local and l-independent representation of the DPP due to specific coupled channels, is as follows: a coupled channel (CC), coupled reaction channel (CRC) or projectile breakup breakup (BU), calculation yields an elastic channel S-matrix S_l or S_{lj}. Inversion of this S-matrix yields a complex inverted potential $V_{\rm inv}$, with spin-orbit terms where relevant. Subtracting the diagonal potential of the CC calculation, $V_{\rm bare}$ (the "bare" potential), from $V_{\rm inv}$ yields a local and l-independent representation of the DPP, $V_{\rm DPP}$ due to the specific included channel coupling effects. The inversion is usually very exact so that the sum $V_{\rm bare}+V_{\rm DPP}$ is a local potential that exactly reproduces the elastic scattering S-matrix from the CC calculation. In the case that the parameters of the CC calculation are fitted to elastic scattering data, $V_{\rm inv} = V_{\rm bare}+V_{\rm DPP}$ is a potential that fits that data. It is therefore appropriate for comparison with phenomenological local potentials. The almost universal undularity in the DPPs determined in this way is relevant to the l-dependence of the OMP. The DPP could in principle be calculated using Feshbach's formalism, refs. [11, 12,27,30], but a conversion to a local and l-independent form, suitable for comparison with phenomenological systematics, has seldom been attempted.

In sect. 6.2 we report fairly recent calculations of DPPs for scattering of nucleons from a range of nuclei from ^{6}He to ^{40}Ca. We omit discussion of earlier works that were carried out before recent computational and coding developments that yield more exact CRC, calculations. Two general conclusions apply to all the results: i) the DPPs are never proportional, point by point, to the bare potential, for an example see fig. 5 discussed below, and ii) the DPPs are generally undulatory to varying degrees, often having radial ranges where the imaginary term is emissive. In some cases the full inverted potential, $V_{\rm bare} + V_{\rm DPP}$, has local emissive regions without breaking the unitarity limit $|S_l| \leq 1$; the CC calculation itself satisfies this limit. These properties are relevant to the question of l dependence. Point i) implies that it is a mistake to fit elastic

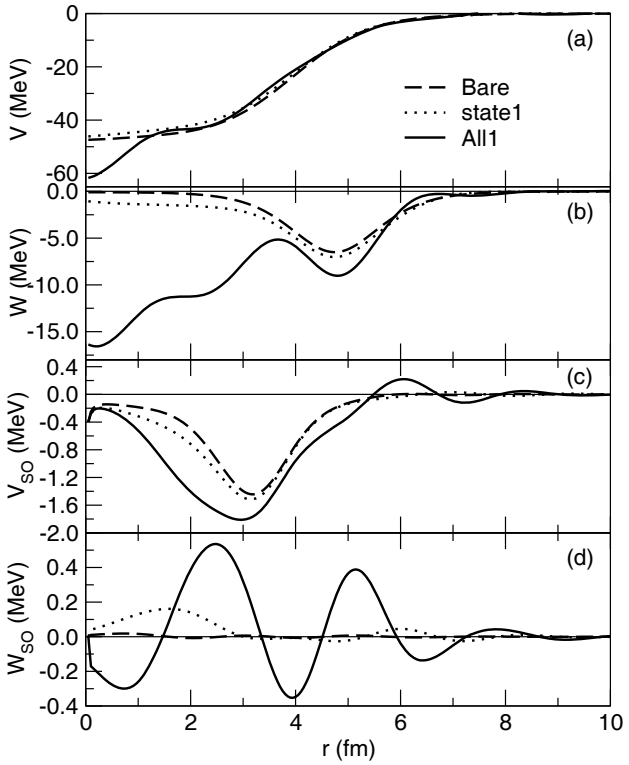

Fig. 5. Potentials generated by coupling to pickup channels for 30.3 MeV protons on ^{40}Ca. From top: real and imaginary central potentials, real and imaginary spin-orbit potentials. The dashed lines are for the bare potentials, solid lines for a full set of pickup states, and the dotted lines are for coupling to the lowest $\frac{3}{2}^+$ state, see refs. [32,34,55,35]. The DPPs are the differences between the dotted or solid lines and the dashed lines (bare potential).

scattering data by uniformly renormalizing folding model potentials.

In sect. 6.3 we review the DPPs arising from the interaction of loosely bound nuclei with target nuclei; both the general properties i) and ii) apply. The inverted potentials and DPPs presented in figs. 7 and 8, for the case of 52 MeV deuterons on ^{40}Ca, show coupling effects that are quite typical for energies well above the Coulomb barrier.

6.2 Survey of DPP results for nucleon scattering

The contribution of neutron pickup channels to the proton OMP for scattering from ^{40}Ca at 30.3 MeV was studied using CRC in refs. [32,34,55,35]. The pickup coupling generated local potentials that are compared with the bare potential (dashed lines) in fig. 5. The dotted lines are for coupling to just the lowest $\frac{3}{2}^+$ state of ^{39}Ca and the solid lines are for coupling to a large set of $\frac{1}{2}^+$, $\frac{3}{2}^+$, $\frac{5}{2}^+$ and $\frac{7}{2}^-$ states.

A conspicuous feature in the real central part is the deep attraction induced by coupling at the nuclear center. However, the overall effect is repulsive, with an overall reduction in the volume integral of 7.4 MeV fm^3 *i.e.* $\Delta J_{\rm R} = -7.44$ MeV fm^3 (volume integrals are given as per nucleon according to the convention of ref. [30].) The rms radius of this component increased by 0.034 fm in part due to undulations in the surface, not apparent on the scale of fig. 5. Reference [35] explores the development of the deep attraction at the nuclear center which is absent when fewer states are coupled. For coupling to just the $\frac{3}{2}^+$ state, the overall reduction in the volume integral of the real part was greater than for the solid line: $\Delta J_{\rm R} = -12.88$ fm^3 and the rms radius was increased by 0.033 fm. Quite apart from the undulatory features, the change in rms radius shows that the coupling cannot be represented as a renormalization. The large magnitude imaginary central DPP was also undulatory in the surface with a localized region near 6.8 fm where it is almost emissive. The real and imaginary spin-orbit terms were conspicuously undulatory, as shown in the lower panels of the figure.

Reference [35] also presents DPPs for neutron scattering from ^{40}Ca at the same energy; the real DPPs for neutrons differ from those for protons, with strong repulsion at the nuclear center. The same reference reveals that undularity of both proton and neutron DPPs decrease as the energy increases from 25 MeV to 45 MeV.

In summary: the effects of coupling to pickup channels could certainly not be reproduced with l-independent potentials having standard forms, or renormalized folding model potentials. In particular, the undularity in the surface region implies l dependence.

The DPP arising from the coupling to vibrational collective states in the same nucleus at the same energy, has strong undulatory features in all components, ref. [36], see fig. 6. With a large set of vibrational states, the amplitude of the undularities in the DPP are large enough point-by-point to be disproportionate to the overall changes in the volume integrals. Unlike the case of pickup coupling, the overall effect on the real central DPP, as measured by the volume integrals, is attractive. The undularity of the imaginary part is comparable to that of the real part, and leads to substantial emissive regions in the complete imaginary potential in the surface (without breaking the unitarity limit). Figure 6 reveals that the DPP for neutron scattering has the same pattern of undulations as for protons, but with somewhat different amplitude. The difference is not due to the absence of coulomb excitation for neutrons.

In ref. [36] the contributions to the OMP of coupling to pickup channels and vibrational states were not included together. However, they were for proton scattering from ^{16}O, ref. [33], which studied the contributions of inelastic and transfer couplings, separately and together, for 30.1 MeV protons. Both couplings generated undulatory DPPs with emissive regions. The undularities generated by pickup and inelastic coupling were quite different.

The contribution to the interaction between protons and ^{6}He due to breakup of ^{6}He, was studied in ref. [111] at c.m. energies of 22 MeV and 35 MeV. For a nucleus of such limited radial extent there is an obvious limit to the possible degree of undularity. The real central DPP is substantially repulsive for r less than ~ 2 fm and attractive in the surface. The imaginary central potential is absorptive

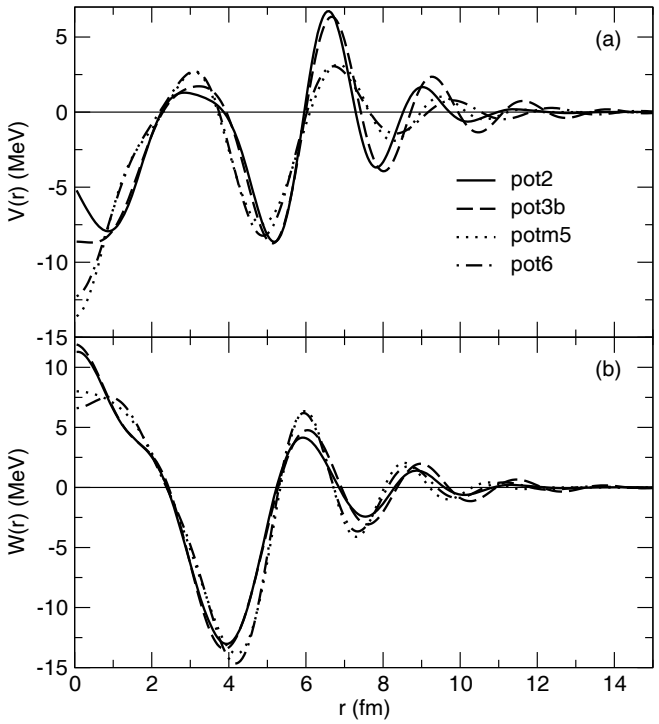

Fig. 6. For 30.3 MeV protons and neutrons scattering from ^{40}Ca, the DPPs arising from the coupling to ten phonons. The solid and dashed lines represent DPPs for two alternative inversion solutions for protons, and the dotted and dot-dashed lines represent DPPs for two alternative inversion solutions for neutrons. Panel (a) gives the real part and panel (b) the imaginary part.

around 2 fm with a tendency to become emissive near the origin and in the surface. The real and imaginary spin-orbit DPPs both change signs from negative to positive at $r \sim 2$ fm. The form of S_{lj} corresponding to this behavior could not occur with an l-independent potential without undulations.

The contribution to the interaction between protons and ^{6}He due to neutron pickup from ^{6}He was studied in ref. [112] at 71 MeV/nucleon. Pickup leading to the $1/2^-$ and $3/2^-$ states were included separately and together. At this energy, the DPPs are more undulatory than for the lower energy case [111] involving breakup of the ^{6}He target. It was found that breakup of the outgoing deuterons significantly modifies the DPPs, reducing the repulsive effect on the real central term, but not enough to modify the overall finding: pickup coupling induces repulsion and absorption in the central term and modifies the spin-orbit terms in a complicated way. The overall effect could not be simulated with without l-dependence in a potential without undulations.

The contribution to the interactions between protons and ^{8}He due to coupling to neutron pickup channels was studied in ref. [113] and, more completely and over a wider energy range, in refs. [31,114]. The DPPs for the most complete calculation [31], designated "d5" at 15.66 MeV/nucleon, have real central terms that were repulsive around 1.5 fm and 4.5 fm and attractive near 3 fm, *i.e.* it is undulatory. The imaginary central term is absorptive for all r, but peaked around 1.5 fm, *i.e.* well within the overlap region. The DPP has substantial real and imaginary spin-orbit terms. At 25 MeV/nucleon, the general shapes of the various terms are similar, although the repulsion in the real central term for low r is greatly enhanced near the origin. For the higher energy of 61.3 MeV/nucleon, the properties are generally similar again but with a marked reduction in the wavelength of the undulations, which are quite substantial out to about 7 fm for the central terms. The spin-orbit DPPs are largely confined to $r \leq 2$ fm. The relevant point once more is that the DPP could not possibly be well represented by a smooth and l-independent potential. In addition, ref. [31] presented arguments that the pickup-induced DPP was dynamically non-local, consistent with theory, *e.g.* [11, 30]. Note that dynamical non-locality is distinct from non-locality due to exchange, and there is no simple correction comparable to the Perey factor for exchange non-locality.

In ref. [115], the contribution of neutron pickup to the proton-^{10}Be interaction was studied at 5 energies between 12 MeV and 16 MeV. For the real central term, a consistent pattern of repulsion near 2.5 fm and attraction near 6 fm was found, with an overall strong repulsive effect as quantified by the volume integral. The appearance of a 0.5 MeV deep attractive region at 6 fm, where the bare potential is very small, indicates that the coupling effect on the real central component could not be represented with a smooth l-independent form. The imaginary central term showed a consistent pattern of emissiveness for $r < 2$ fm and absorption further out. At these lower energies, where undularities have a relatively long wavelength, a reasonable representation by a smooth potential may be possible.

6.3 DPPs for scattering of loosely bound nuclei

The first exact $S_l \rightarrow V(r)$ IP inversions [89] were for breakup of ^{6}Li. The DPPs, exhibited strong repulsion in the surface region, showing explicitly why the folding model for this nucleus required renormalization. Such renormalization was not required when the same folding model was applied to less loosely bound projectiles. An approximate inversion method, weighted TELP (see sect. 2.6) had already been applied and came to the same general conclusion concerning the surface region. However, the weighted TELP method, although approximately correct in the surface region, misses various features, in particular undularities, that appear in exact inversion and which are relevant to the question of l-dependence. Comparisons of weighted TELP and exact inversion can be found in ref. [116]. Exact inversion can provide information concerning the DPP deep into the overlap region. This is significant as found [117] in connection with transfer DPPs for ^{8}He.

Reference [118] determined the DPPs due to the breakup of 80 MeV deuterons on ^{58}Ni and 156 MeV ^{6}Li on ^{12}C. The DPPs were well-determined down to small radii and showed remarkably similar distinctive radial shapes

for deuterons and ^{6}Li. The similarity applied also in the comparison of two breakup models: i) when there was only S-wave breakup, and ii) when D-wave breakup was also included. The strong undulatory form of these DPPs was such that the real part varied with r from substantial surface repulsion to double peaked attraction within the overlap region. The elastic scattering S-matrix responsible for such shapes could not be reproduced with a smooth (non-undulatory) l-independent potential. A later study [119] of the breakup DPP for deuterons on ^{58}Ni, involving more precise breakup calculations for 56, 79 and 120 MeV deuterons, found essentially the same pattern of attraction and repulsion in the real part, and of absorption in the imaginary part. One respect in which the later calculations differed was in the more distinct region of emissiveness in the imaginary part. There is no possibility of the CDCC elastic channel S-matrix being reproduced by a smooth l-independent potential.

Reference [116] presented the DPPs due to the breakup of ^{6}Li on ^{12}C at 90, 123.5, 168.6, 210 and 318 MeV with parameters adjusted to fit elastic scattering angular distributions at each energy. At the highest energy, a notch test indicated sensitivity down to a radius of about 2 fm. The DPPs were consistent with those found in the earlier less rigorous calculations of ref. [118]. Reference [116] also reported a comparison of weighted TELP inversions and precise S-matrix inversions, revealing the limitations of the former. In particular, weighted TELP failed to get the magnitude of the DPP correct in the outer radial regions and entirely missed significant structure at smaller radii, where the notch test indicated sensitivity.

There is much interest in the interaction of loosely bound nuclei with heavier nuclei at energies near the Coulomb barrier. This situation presents difficulties for inversion calculations, but the study [120] of ^{8}B, ^{7}Be and ^{6}Li on ^{58}Ni at energies near the Coulomb barrier did present DPPs for ^{8}B and ^{7}Be. The DPP for ^{8}B differed from that for ^{7}Be, but both the real and imaginary parts had general features in common. In both cases the real part had a very long attractive tail that became repulsive further in. In each case there was a long absorptive tail which for ^{7}Be had a wavy feature, but became emissive for $r < 9$ fm whereas the imaginary part for ^{8}B remained absorptive. The case of 170.3 MeV ^{8}B on ^{208}Pb, involving the coupling to breakup channels, was more amenable to inversion, ref. [121]. In this case the real DPP had long range attraction, becoming repulsive for $r < 15$ fm. The imaginary DPP had a long absorptive tail, becoming emissive for $r < 11$ fm. Currently achievable experimental elastic scattering angular distributions would probably be insensitive to these details. Nevertheless, any smooth potential reproducing the CDCC elastic channel S matrix would necessarily be l-dependent.

For 52 MeV deuterons scattering from ^{40}Ca, the combined contribution to the deuteron-nucleus potential due to the coupling to ^{3}H and ^{3}He pickup channels and also deuteron breakup channels, was studied in ref. [122]. In certain cases, see below, coupling to proton channels (stripping) was also included. The selected processes were included together in CRC calculations in which the bare

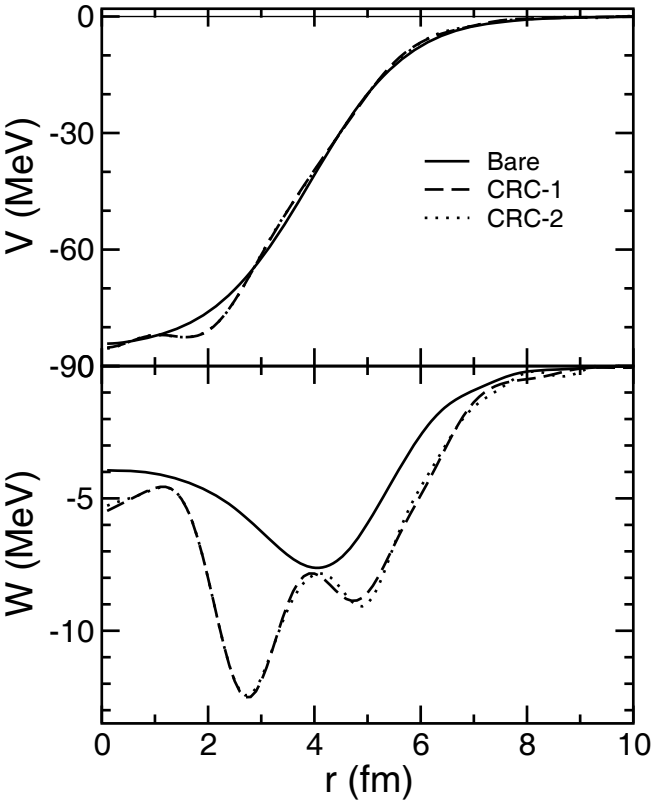

Fig. 7. For 52 MeV deuterons on ^{40}Ca, real and imaginary central potential, real part above and imaginary part below. The solid lines are the bare potential and the dashed and dotted lines are for two alternative inversions, as described in the text, of the elastic scattering S-matrix when full channel couplings, apart from stripping, are switched on.

OMP was adjusted to optimise the fit to the elastic scattering angular distribution. The (d, t) angular distributions were also fitted. When stripping was included, vector and tensor analysing powers were calculated, enabling the contribution of the coupling to the spin orbit and T_R tensor interactions to be determined, although experimental data to compare with these are lacking. It was shown that the complex, central contribution to the DPP was well established, and that is briefly summarized here.

Although spin-1 inversion of $S^{J}_{l'l}$ leading to the T_R interaction is possible, and results of this were presented in ref. [122], it is also of interest to test the possibility of a suitable J-weighted inversion, which leads to reasonable central terms, and is applicable in cases where full spin-1, or spin-$\frac{3}{2}$, inversion is unavailable. Figure 7 compares the bare potential with two inverted potentials calculated with J-weighted inversion. The inverted potential shown as dotted lines has a closer fit to the S-matrix (technically, a lower inversion-σ, see eq. (7) and refs. [87, 69,75]). The contribution to the real part appears small in this figure, but when the bare potential is subtracted from the inverted potentials, it can be seen that the real DPP is comparable in magnitude to the imaginary DPP, as shown in fig. 8. In this case the imaginary DPP is quite substantial compared to the imaginary bare term, and is

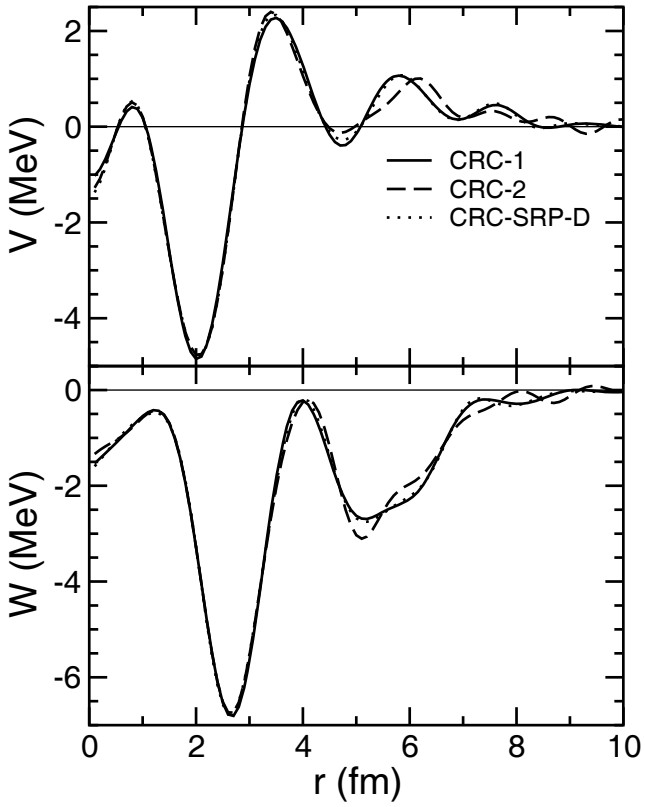

Fig. 8. For 52 MeV deuterons on ^{40}Ca, real and imaginary central DPPs found by subtracting the bare potential from the inverted potential, real part above and imaginary part below. The solid and dashed lines correspond to the dashed and dotted lines of fig. 7 and the dotted lines are for a third, alternative, inversion, see ref. [122].

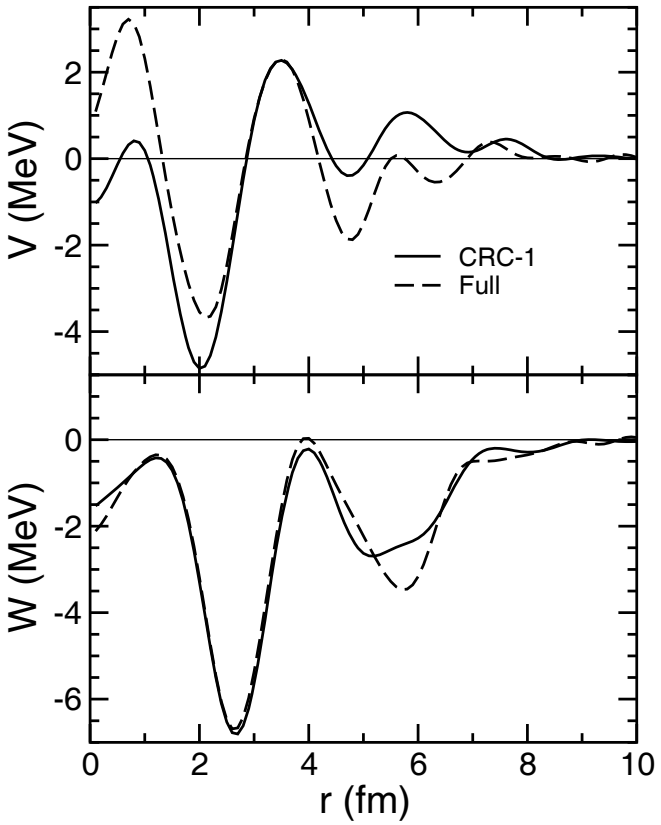

Fig. 9. For 52 MeV deuterons on ^{40}Ca, real and imaginary central DPPs found by subtracting the bare potential from the inverted potential, real part above and imaginary part below. The solid line is as for the solid line in fig. 8 and the dashed line is for the central terms of the "full", *i.e.* not J-weighted, inversion.

everywhere absorptive; this is by no means always the case with reaction channel coupling. The relevant point is that the radial shape is strongly undulatory, as typical when reaction channel coupling is included. No smooth l-independent potential could reproduce the S-matrix. The J-weighted inversion gives generally reasonable results as can be seen in fig. 9 where the dashed lines represent the central potential from a full spin-1 inversion. The imaginary part is little affected and actually becomes less absorptive at 4 fm, becoming slightly emissive there. The real part is substantially modified for $r < 2$ fm and also around 6 fm.

The DPP when stripping channels are included in a more complete CRC calculation is presented by the solid lines in fig. 10. The imaginary DPP is more absorptive for most values of r, but becomes more undulatory in the surface region, with distinct excursions into emissiveness. The dot-dashed lines for the central terms in fig. 10 are the same as the dashed lines in fig. 9.

In summary, for the cases described here, with the possible exception of the lowest energy cases (for protons on ^{10}Be), *an l-independent potential model representation of the elastic scattering S-matrix, when reaction channel or inelastic coupling is included, requires an undulatory potential.* The fact that, as will be shown, a potential that is S-matrix equivalent to an l-dependent potential will be undulatory strongly suggests that l-dependence and undularity are alternative representations of the channel coupling effects that contribute to elastic scattering interactions.

6.4 Alternative representation of DPPs

So far, we have considered potentials that were functions $V(r)$ of radius r, and were determined by the S-matrix elements S_l or S_{lj}. If these S-matrix elements are the product of a CC calculation, then subtracting the bare potential $V_{\rm bare}(r)$ leads to a DPP that is a function of r. There is an alternative: one can determine the potential that yields exactly the elastic channel radial wave functions $\psi_{lj}(r)$ for all partial waves lj. When there is no channel coupling, the result will be a function of r only: the angle-independent bare potential $V_{\rm bare}(r)$ is reproduced. But when there are channels coupled to the elastic channel, the resulting potential will no longer be a function of r only, but also depend upon the angle in the scattering plane. When there is coupling, the effective elastic channel local l-independent potential is non-spherical $V(\mathbf{r})$. The

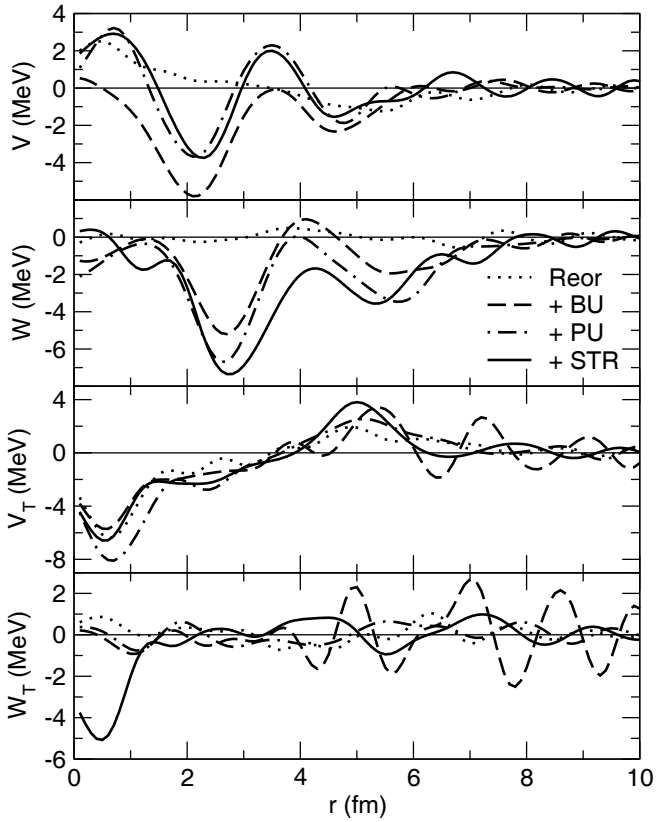

Fig. 10. For 52 MeV deuterons on ^{40}Ca, DPPs for complete coupling including pickup. From top, real central, imaginary central, real tensor T_R, imaginary tensor T_R. For the complex spin-orbit terms, see ref. [122]. Included coupling: dotted lines, reorientation only; dashed lines add deuteron breakup; dot-dashed lines add pickup to ^{3}He and ^{3}H; solid lines include also stripping to states of ^{41}Ca. The dot-dashed lines for the central terms correspond to the dashed lines in fig. 9.

difference between these "ψ-potentials" will be a spatial representation of the DPP depending on θ as well as r.

An account of this procedure and examples of its applications can be found in refs. [123–127]. In ref. [124] it was shown explicitly how the ψ-potential representing an l-dependent potential becomes oscillatory along the line of zero impact parameter. The later references presented the ψ-potential on the entire scattering plane. Reference [126] presented ψ-potentials for the elastic scattering wave function for cases of vibrational coupling and coupling to pickup channels. In each case, the ψ-potential was very non-spherical, the imaginary part typically having emissive regions even when the potential was overall absorptive.

One test in ref. [126] shows that the reduction in the magnitude of the spatial wave function $\psi(r, \theta)$ due to Perey-Buck [63] non-locality, had a small dependence on θ and the magnitude predicted by Perey [128] for r in the nuclear interior. This verified both the conventional Perey factor and the formalism for calculating the ψ potentials.

Where there is channel coupling, the situation is very different. The DPPs have a substantial angular dependence as well as a complex radial dependence. Reference [126] presents a "generalized Perey factor", GPF, the ratio at point r, θ, ϕ (for $\phi = 0$ and $\phi = \pi$) between the magnitude of an elastic channel wave function ($\psi(r, \theta, \phi)$), typically from some CC calculation, and the magnitude of the wave function for the local l-independent potential found by inverting the elastic channel S-matrix. This ratio expresses the reduction or enhancement of the magnitude of the elastic channel wave function over the scattering plane and varies greatly from point to point, showing that dynamical non-locality behaves in a very different way to exchange non-locality with its fairly uniform effect within the nucleus. This is not surprising in view of the undulatory form of the DPPs calculated by inversion. Clearly, no smooth l-independent potential could yield the angle-dependent ψ-potentials derived directly from the elastic channel wave functions of CC calculations. They constitute an alternative representation of the l-dependence and dynamical non-locality due to channel coupling.

6.5 Consequences for phenomenology

Empirical study requires precise model-independent fits to wide angular range elastic scattering data. Such model-independent fitting should *not* be terminated at the point when precise fits imply undulatory potentials, cf. ref. [99]. The evaluation of folding model potentials must not simply involve a search on a normalization constant to optimize the fit, but should determine an additive radial form by model independent fitting. For energies near the Coulomb barrier, the properties of the DPP are rather abstract since the details are difficult to relate to experiment. Nevertheless, the properties found for such low energy DPPs contribute to a systematic understanding of l dependence generated by channel coupling.

7 l dependence and its connections to reaction theory

Inversion implies that l dependence and undularity are alternative representations of dynamical processes that contribute to nuclear scattering. Similarly,. phenomenology makes it clear that l dependence and undularity are alternative representations of potentials that fully and precisely represent high quality elastic scattering data. There is as yet no comprehensive answer to the relationship between such data-fitting representations and the dynamics of nuclear interactions. With a comprehensive picture lacking, we report on relevant cases that have been studied.

7.1 Relating l dependence to the effects of channel coupling

Given a purely phenomenological l-dependent potential, how is this l dependence related to the contributions to

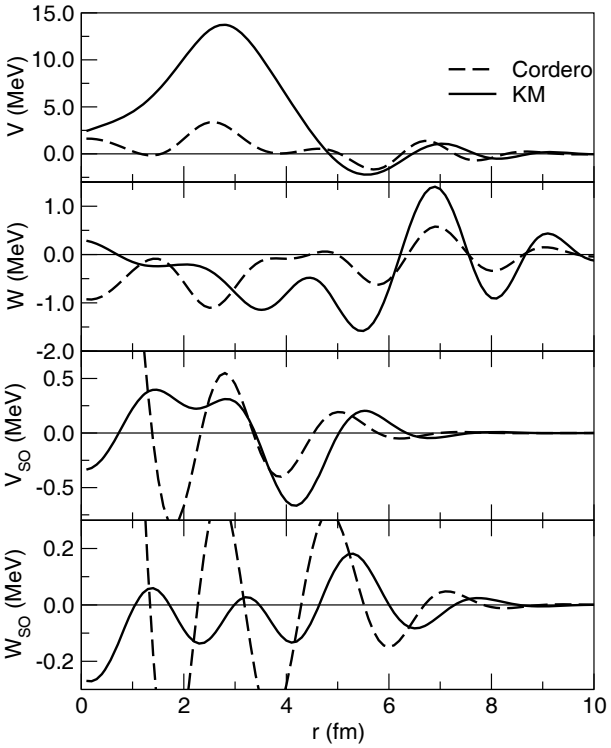

Fig. 11. For 30.3 MeV protons on ^{40}Ca, the four components of the l-independent equivalent of the full l-dependent potential of ref. [103] (dashed lines) and of ref. [104] (solid lines) with, in each case, the respective l-independent part of that potential subtracted. From the top: the real central, imaginary central, the real spin-orbit and imaginary spin-orbit components.

the elastic channel potential from inelastic and reaction channels as evaluated by $S_l \rightarrow V(r)$ inversion? This question can be approached by directly comparing the changes in $|S_{lj}|$ and $\arg(S_{lj})$ that are due to channel coupling with the changes in these quantities arising from the l-dependent terms. This was done in ref. [56] where a qualitative similarity was found. Alternatively, invert S_{lj} from the empirical l-dependent potential and compare the properties of the resulting l-independent potential with those of potentials found by inverting the elastic channel S_{lj} from the coupled channel calculation.

We first compare the two phenomenological cases of sect. 5.2, ref. [103] and ref. [104], subtracting from the (wavy) l-independent potentials, which were determined by inverting S_{lj} from the l-dependent potentials, the respective (smooth) l-independent component of the corresponding l-dependent potential. We associate the wavy difference potential with the l dependence. Figure 11 compares two cases: the dashed lines are for the l-dependent potential of ref. [103] ("Cordero" in the figure) and the solid lines are similarly for ref. [104] ("KM" in the figure). Each parameter search fitted both the l-independent and l-dependent components so the curves do not involve subtracting the same l-independent terms.

There are common properties, beyond the simple fact of undularity. The surface region is significant, and the "wavelength" of the undulations is the same in each case. For the real central terms the amplitude is greater for the KM case reflecting the superiors fit to the data. A significant feature, as noted in sect. 5.2 above, is the existence of emissive regions in the imaginary central term near 7 fm and 9 fm. These persist in the full (unsubtracted) potentials. Such emissivity, having restricted radial range and not breaking the unitarity limit, commonly arises both as a result of channel coupling and also in phenomenological l dependence, as here. For $r < 5$ fm, the central terms for both the solid and dashed lines, the Cordero and KM cases, exhibit repulsion and absorption. This is also a general characteristic of the coupling to deuteron channels, as shown by the DPPs from the CRC calculations of refs. [32, 34,55,35]. These DPPs, generated by pickup coupling, also exhibit emissive regions in the central imaginary term at 7.5 fm (see fig. 5) and 9.5 fm (not shown in refs. [32,34, 55,35] for 9.5 fm.) The KM and Cordero spin-orbit components have a generally similar undularity, with repulsion around 6 fm in the real terms and emissivity for both imaginary parts around 5 fm.

Although the DPPs from the pickup coupling calculations show similar undularity in the surface region, for $r < 6$ fm, to that arising from l dependence, the DPPs for the central terms in refs. [32,34,55,35] and fig. 5 are relatively smooth, exhibiting repulsion in the real part and absorption in the imaginary part. However, pickup channel coupling is not the only coupling that might lead to l dependence. References [44,45] cited previously demonstrated that coupling to giant resonances had a significant effect. This effect was directly compared in ref. [45] with the contribution to S_{lj} of the phenomenological l-dependent term for just $|S_{lj}|$ but unfortunately not for $\arg(S_{lj})$, which is most directly related to the real part of the potential. In ref. [36] the DPP due to coupling to a large set of phonons for 30.3 MeV protons on ^{40}Ca had emissivity in the imaginary part near 6 fm and 9 fm, and quite large amplitude undulations over the full radial range, see fig. 6. As mentioned in sect. 5.2, the l-independent equivalent to the empirical l-dependent potential does have emissive excursions in the surface imaginary term that match the surface emissivity, among other features, of this phonon-induced DPP quite well.

There have been few realistic calculations of the DPP including both reaction channels and collective states together. An exception is ref. [33] in which pickup and collective contributions to the proton and neutron interactions with ^{16}O are studied. Nucleon interactions with ^{16}O are discussed sect. 7.4. We would hope in future to have realistic comparisons between the local l-independent equivalents to both i) potentials derived from comprehensive channel coupling, and, ii) l-dependent potentials that precisely fit elastic scattering data at the same energy. At present we can only observe qualitative similarities.

7.2 Relating model-independent potentials to l-dependence.

Reference [98] presented l-independent potentials fitted to elastic scattering angular distributions and analyzing pow-

ers for protons scattering from ^{16}O and ^{40}Ca for various energies. These model independent fits using spline functions were described as "theoretically unprejudiced fits" although it is now clear that a prejudice was imposed: the prejudice that the imaginary part of the potential should be absorptive everywhere. It is now understood that this is not a necessary condition for $|S_{lj}| \leq 1.0$ (the unitarity limit) and oscillatory imaginary potentials can have localized emissive regions without breaking the unitarity limit. Moreover, as mentioned in sect. 5.1, the lack of suitable Wolfenstein (spin rotation) data makes fully unambiguous theoretically unprejudiced fits formally impossible for proton scattering. However, model independent fitting absolutely requires wavy potentials, and the waviness found for the case of ^{40}Ca does share some features with that in fig. 11, in particular repulsion near 3 fm. Phenomenology based on fits at a single energy is further complicated by the possibility of "transparent potentials", *i.e.* (highly undulatory) potentials that, when added to another potential, make effectively zero change to S_l or S_{lj}.

In sect. 5.1 we referenced other precise model independent fits that led to wavy potentials, refs. [96,97,99]. We currently lack the means to establish a comprehensive relationship between specific channel couplings and the (wavy) l-independent potentials fitted to data.

7.3 Model calculations linking l dependence and undularity

The DPP generated by coupling to specific channels, as determined by S-matrix inversion, is generally undulatory. This waviness is not an artefact of inversion and is not restricted to proton scattering, but also applies to the coupling to breakup channels for composite projectiles. For ^{6}Li scattering on ^{12}C, CDCC breakup calculations [116] revealed a tendency for the local DPP due to ^{6}Li breakup to be somewhat wavy in the surface for the lowest energy (90 MeV) case.

Calculations [119] of deuteron breakup on ^{58}Ni revealed that, surprisingly, $|S_l|$ often increases as a result of processes presumed to remove flux from the elastic channel. When that study was extended down to 50 MeV, a significantly undularity appeared in the surface region of the inverted potential. The wavy form of the DPP does not correspond to the radial shape of the excitation or transfer form factor and the undulations make a nearly zero contribution to the volume integral.

To get some understanding of these undulations, simple model calculations for 50 MeV deuterons on ^{58}Ni were performed. A basic question was posed: given S_l calculated from an l-independent potential, what l-dependent modification of this S_l might give rise to undularity of the kind that has been found? This aspect of potential scattering theory has had little attention. The argument, $\arg S_l = 2\delta_l$, and modulus, $|S_l|$ of the S-matrix $S_l = \exp(\mathrm{i} \arg S_l)|S_l|$ calculated from a standard WS potential were independently modified ($\arg S_l$ and $|S_l|$ relate mostly to the real and imaginary parts of the potential respectively) and the new S-matrix was inverted. The modifications were such that S_l was unchanged for lowest l and either $|S_l|$ or $\arg S_l$ was modified for high-l, with a smooth transition. In both cases the inverted potential had undulations: these had a larger amplitude in the real part when $\arg S_l$ was modified and a larger amplitude in the imaginary part when $|S_l|$ was modified. The modification of $\arg S_l$ had a much larger effect on J_{R} than on J_{I} and effectively *zero* effect on the total cross section although the elastic scattering angular distribution *was* modified significantly. That is, *a large modification in the angular distribution was accompanied with essentially zero change in the total reaction cross section.*

The modification of $|S_l|$ was such that, $(1 - |S_l|)$ was multiplied by

$$f_{\mathrm{m}}(l) = 1 + z_{\mathrm{m}} \frac{1}{1 + \exp((l - l_{\mathrm{m}})/a_{\mathrm{m}})} \tag{9}$$

for $l_{\mathrm{m}} = 14$, $z_{\mathrm{m}} = 0.1$ and $a_{\mathrm{m}} = 2$ with the asymptotic effect: for $l \ll l_{\mathrm{m}}$, $|S_l| \to |S_l|$, for $l = l_{\mathrm{m}}$, $1 - |S_l| \to (1-|S_l|) + \frac{z_{\mathrm{m}}}{2}(1-|S_l|)$, and for $l \gg l_{\mathrm{m}}$, we have $1-|S_l| \to (1 + z_{\mathrm{m}})(1 - |S_l|)$.

The effect of this was to increase the volume integral of the imaginary part of the inverted potential, J_{I}, and increase the reaction cross section. It also induced Fraunhofer-like oscillations on the elastic scattering angular distribution. The effect was linear insofar as, for example, all these effects changed sign for $z_{\mathrm{m}} = -0.1$. When the modified S_l was inverted, the most relevant effects were: i) very strong oscillations appeared in the imaginary potential, ii) oscillations also appeared in the real part but these corresponded to very small changes in the volume integral J_{R} and rms radius, iii) the oscillations in the imaginary part in the surface included excursions into emissivity. There was no question of the unitarity limit being broken since the modification of $|S_l|$ did not allow that. For a fuller account of the model calculations, see [129].

In sect. 8 we will associate strong undulations with a rapid change in S_l around the l values for which $|S_l| \sim \frac{1}{2}$, and that is supported by the above results. Moreover, waviness does not occur in just one (real or imaginary) component. Point iii) is significant, telling us not to exclude, on unitarity grounds, the occurrence in model independent fits of local radial regions where the imaginary component is emissive.

7.4 Reaction theory and proton scattering from ^{16}O

The remarkably precise wide angular range data for angular distributions and analysing power for proton scattering from ^{16}O from about 20 to 50 MeV have led to many attempts have been made to fit them. This includes spline fitting [98] in which precise fits led to undulatory potentials (but see comments in sect. 7.2). The data were also well fitted with an l-dependent potential [104] with smoothly varying characteristics. For 30.1 MeV protons, comparing l-dependent and l-independent fits, χ^2/N for the angular distribution was two orders of magnitude lower for the l-dependent fit and for the analysing power one order of magnitude lower for the l-dependent fit. While

short of the $\chi^2/N \sim 1$ target, the consistency of the potential over the range of energies and the vast superiority over conventional Woods-Saxon fitting, was conspicuous. However, these results were obtained before the parity dependence of the proton-^{16}O interaction, due to exchange processes, was established. This parity dependence was manifest in the inversion of S_l from RGM calculations for protons up to 25 MeV, ref. [83]. The Majorana term of the inverted potential was strongly repulsive for $r < 2$ fm to an extent that was less at around 25 MeV than at zero energy. The sign of the Majorana term is opposite to that for the proton-^{4}He interaction and, as expected [70], less in magnitude.

The RGM results are consistent with the most comprehensive fits to elastic scattering data: a good fit to the high quality angular distribution and analysing power data over a wide range of energies, was achieved by Cooper [84] using direct data-to-potential energy-dependent inversion. Single energy fits were also found with χ^2/N values ranging from about 3 to about 9 for energies from 27 to 43 MeV, far lower than for conventional phenomenology, although greater than for precision single-energy model-independent fitting. From this work there emerged a complex, parity-dependent potential, that was remarkably consistent over the whole energy range studied. Two features stand out:

i) the real central Majorana term is repulsive for small r and attractive further out, remarkably like the Majorana term found by inverting the RGM S_l, ref. [83].
ii) the imaginary central term is strongly emissive for $r <$ 2 fm.

The second feature would certainly require an l-dependency in order to be represented by a conventional smooth potential.

For nucleons scattering from ^{16}O the local equivalent contributions of coupled collective states and also reaction channels (pickup channels) have been determined separately and together [33]. Undulatory DPPs were found and there was a substantial difference in the pickup DPPs for protons and neutrons, mostly due to different Q-values and transfer form factors for (p, d) and (n, d) processes. There were emissive regions in the DPPs.

Theoretical and empirical evidence both imply that the proton plus ^{16}O potential certainly has both significant parity dependence, and also dynamical l dependence. Any phenomenological treatment of the proton plus ^{16}O system that ignores parity dependence is therefore deficient, as is any treatment ignoring the l-dependence arising from coupling to inelastic and transfer channels.

7.5 Reaction theory and proton scattering from ^{40}Ca

Section 2.6 referred to the old problem of fitting proton scattering from ^{40}Ca. In a paper from 1967 by Gross *et al.* [130] we read: "The ^{40}Ca nucleus has for some time been recognized as a bête-noire of the optical model. [...] It proved to be impossible to fit the scattering data beyond 140° and obtain a simultaneous fit to the polarization and cross-section data with a reasonable set of optical-model parameters." Nearly 50 years later there is no generally agreed solution to the problem of proton scattering from ^{40}Ca, but there is clear evidence that l dependence is involved. The l-dependent fit of ref. [104] for 30.3 MeV protons gave $\chi^2/N = 2.09$ for the angular distribution compared with the best for a conventional Woods-Saxon fit of $\chi^2/N = 20.25$, with somewhat less improvement for the analysing power. Parity dependence will be much less for ^{40}Ca than for ^{16}O [70].

Initially [54], coupling to deuteron channels appeared to solve the problem of the backward angle dip, but as the calculations became more complete this agreement disappeared. Most recently [35], the DPP arising from coupling to a large set of pickup states has been determined; it is not remotely of a form that would smoothly correct a folding model potential. It was not adjusted to fit the elastic data since fitting data with a large collection of coupled reaction channels was challenging at that time. A meaningful fit to data would also require the inclusion of the collective states. As noted in sect. 6.2, coupling to a large array of collective states made a large contribution [36], but there is no full calculation that precisely fits the data. Thus, although the calculations showed the power of channel coupling to modify backward angle scattering, they are very incomplete. What emerged from ref. [36] is that the local equivalent DPP generated by coupling a plausible large collection of collective states is notably undulatory, and, as remarked above, exhibits a large emissive feature in the imaginary part for $r < 2$ fm. The model independent phenomenological fits of ref. [98] exhibited undulatory features but with a different wavelength. In summary, coupling to both pickup states and collective states generates distinct but very substantial departures from smoothness. Determining the combined DPPs remains a task for the future, requiring fitting the bare potential to the differential cross section and analysing power data in the presence of a large collection of collective and pickup channels.

Fitting the data without coupling is, of course vastly easier, but should not involve a restricted parameterization. Section 5.1 referenced a model independent fit to the 30.3 MeV data by Alarcon *et al.* [99]. The deep backward angle minimum was not fitted; restrictions had been imposed on the model independent fitting to ensure that the radial form was free of undulations.

The characteristic deep, hard to fit, large angle minimum in the angular distribution for elastic proton scattering from ^{40}Ca is probably related to the small number of competing processes for the closed shell nucleus. If l dependence is established for ^{40}Ca, it would be a general property, for nuclei for which it is easier to fit large angle elastic scattering data.

7.6 Scattering theory and low energy neutron scattering

Low energy scattering of neutrons from the doubly closed shell nucleus ^{208}Pb is of special interest as a testing ground

for potentials that are consistent with dispersion relations over a wide energy range, as indicated in sect. 2.8. Studies of this system have revealed evidence for l dependence of a form distinct from all those discussed above. Such l-dependence appears first in refs. [131,132], a study of neutron elastic scattering on ^{208}Pb for energies between 50 and 1005 keV. This work presents evidence for l-dependence in the real part of the potential involving very few partial waves with specific resonant states playing a role.

A larger number of partial waves were involved in the wide energy range study of n + ^{208}Pb elastic scattering [133]. The data were fitted with a potential model that was consistent with causality and which had fixed geometric parameters. At the lowest energies, it was necessary to apply a form of l-dependence which was different from those presented elsewhere in this review. This l dependence applies in a regime where relatively few partial waves are involved. The partial waves $l = 0$ to 6 were divided into two groups, group b containing $l = 1, 3$, and 6, with the remainder in group c; this is clearly not parity dependence. The imaginary surface potential was different for groups b and c with the dispersion relations introducing a corresponding l dependence for the real surface potential. The l dependence, which applies below 12 MeV and down to negative energies, improves the fit at those energies.

A later paper, ref. [134], applied a similar idea but based on a somewhat different grouping of partial waves. In this case the grouping was based on the different relationship between the radial position of the antinodes of the partial waves and the maximum magnitude of the surface imaginary potential. This is clearly reasonable, but depends upon the certainty with which radial parameters of the imaginary part are determined. There may well be a higher order effect in that coupling to inelastic channels, which in a macroscopic picture involves derivatives of the potentials, will be dependent on the form of the imaginary potential. Furthermore, in situations where there are few operative partial waves, the coupling effects for individual partial waves are less likely to average out.

The l-dependent model of ref. [133] was further developed in ref. [135] for n + ^{208}Pb elastic scattering for energies between -20 MeV and 20 MeV. In this case the l dependence allowed good fits when the radial form of the potentials were energy independent. The authors note that a dependency of the imaginary part upon angular momentum is equivalent to a form of non-locality that is distinct from that due to exchange, citing [27]. At this point contact is made with a recurring theme of the present review.

It is hard to relate these low energy cases, involving specific partial waves that are related to specific bound nucleon orbitals, to the forms of l dependence involving many partial waves. As with all l dependence, an alternative representation of the elastic scattering involving an undulatory l-independent potential is possible, but this would not be equivalent when applied in reactions.

8 Scattering of heavier nuclei

There is substantial literature concerning l dependence in heavy-ion scattering with independent arguments that apply to l dependence of the real or imaginary components. Results in sects. 8.1 and 8.2 suggest that when the real and imaginary parts of a potential have different sources of l dependence, the consequences of the l dependence of the real and imaginary terms persist in the complete l-independent potential found by inversion. In sect. 8.3, l dependence due to strong inelastic coupling is discussed for heavier nuclei.

8.1 l dependence due to antisymmetrization

An example of l dependence in the real part is provided by the RGM calculations of Wada and Horiuchi [136,137] for ^{16}O + ^{16}O elastic scattering. The l dependence arises from exchange terms that go far beyond the 1-particle knock-on exchange. Horiuchi [138] reviews such calculations in the context of a more general discussion of microscopic nucleus-nucleus potentials. There is no possibility in this case of there being Majorana terms, although such terms will arise when the interacting nuclei are not identical bosons. The S_l corresponding to the l-dependent real potentials of Wada and Horiuchi were inverted [139] to yield an l-independent potential which is significantly different at lower energies from that derived [136,137] using WKB inversion. The difference between the complete l-independent equivalent potential and the l-independent (non-exchange) part of the refs. [136,137] potential is most marked in the nuclear interior. Such l dependence would therefore be less significant for a potential that includes an absorptive term. Nevertheless, refs. [136,137] established that exchange processes lead to an l dependence of nucleus-nucleus interactions that is in addition both to possible parity-dependence and also to contributions from knock-on exchange.

The model of Kondo *et al.* [140], for ^{16}O + ^{16}O scattering over a range of energies, included a phenomenological l-dependent real term inspired by the model of Wada and Horiuchi, together with an l-dependent imaginary term of the form discussed in sect. 8.2 below. The S_l for the potential with both terms l-dependent was inverted [141] leading to a real potential with a very similar shape and energy dependence to that found [139] for the Wada-Horiuchi potential.

The l dependence of the real part of the Kondo *et al.* [140] potential was an overall factor $V_0 + V_l l(l+1)$, *i.e.* a more gradual l dependence than the sharp transition involving a Fermi form employed elsewhere: $1/\{1 + \exp[(l - l_c)/\Delta]\}$. This, by design, leads to a very similar energy dependence for the l-independent potential found by inverting the Wada and Horiuchi [136] S-matrix. The imaginary part of the potential was of Fermi form as in sect. 8.2 below, but in the 59 MeV case, l_c was 19, rather higher than $kR_W = 12.7$ where R_W is the effective radius defined by Kondo *et al.*. In test cases, it has been found that a sharp transition in the potential for l close to the

value for which $|S_l| \sim 0.5$ consistently leads to an undulatory equivalent potential, generally more undulatory than those found [141] from the S-matrix of ref. [140]. That exemplifies an apparent systematic qualitative difference between the equivalent l-independent potentials found for these "gradual" l-dependencies and the sharper Fermi-form l-dependencies. The latter, especially for sharp changes in the imaginary term, generate more oscillatory equivalent potentials.

The l-independent potentials S_l-equivalent to the Kondo potential had substantially non-zero radial gradients at the nuclear centre (cusp-like) and very different wave functions in the overlap region.

8.2 l dependence due to reduced absorption for high-l partial waves

Following arguments of Chatwin, Eck, Robson and Richter (CERR) [142], explicit angular momentum dependence was introduced into the imaginary part of the OMP for heavier ions such that the absorptive term was reduced for the highest partial waves. This was justified, with reference to Feshbach's theory, on the grounds of the reduced number of channels available for absorption for these partial waves.

This CERR approach has had some success and has been applied in various cases, not all confined to heavier ions. The first applications involving alpha particles gave consistent improvement to α-particle elastic scattering below 20 MeV [143]. A CERR term was incorporated in the analysis by Bisson *et al.* [144] of α scattering from ^{40}Ca in a study in which compound elastic scattering also played a key role. In this particular implementation, the imaginary term was a standard Woods-Saxon derivative form multiplied by the l-dependency,

$$F(l) = \frac{1}{1 + \exp((l - l_c)/\Delta_l)} \tag{10}$$

where, following CERR, $l_c = \bar{R} \times [E_{\rm CM} + \bar{Q}]^{\frac{1}{2}}$. In this case $\bar{Q} = 0$ and $\bar{R}$ was chosen close to the interaction radius. The high l cutoff was quite broad, with $\Delta_l = 4.0$. Reference [144] implies that this l dependence, together with an incoherent compound elastic component, was essential for achieving a reasonable fit over the energy range, 5.5 to 17.5 MeV.

More often, a CERR term has been included for heavier ion scattering such as the model of Kondo *et al.* [140]. Inversion reveals, ref. [141], that except at the highest energy, the l-independent equivalent of the imaginary part has a radial form radically different from that of any l-independent potential found by fitting data. The CERR term was included together with a parity-dependent real potential for ^{16}O + ^{20}Ne scattering by Gao and He [145] and the resulting S_l were inverted [146] to produce an l-independent representation. The resulting imaginary potential was qualitatively similar to that produced [141] by the model of Kondo *et al.* [140].

In ref. [147], CERR l-dependence applied to ^{6}Li scattering from ^{40}Ca led to an improvement to the fit at backward angles. Reference [147] included a comparison of the number of exit channels as a function of exit channel angular momentum for scattering from ^{44}Ca. The result supports the apparent requirement for CERR l-dependence for ^{6}Li scattering from closed shell nuclei. For such nuclei the fewer high-l exit channels is in line with the basic CERR hypothesis. In fact, the formulation of CERR [142] was in terms of the conserved quantity J, the total angular momentum. For zero target and projectile spins, $J = l$, but for the scattering of ^{6}Li the difference is significant, especially where vector analysing powers are to be fitted, as in ref. [148]. In that case the fit to the analysing powers was improved by the inclusion of what, in this case, was J dependence following eq. (10) applied to J rather than l. Another example is ref. [149], in which J-dependent absorption was included together with a tensor interaction to fit a full set of tensor, as well as vector, analysing powers in polarized ^{6}Li scattering from ^{12}C.

Reference [68] shows how the energy dependence of the CERR l-dependent cutoff leads, by way of dispersion relations, to an l dependence in the real potential for ^{16}O + ^{16}O scattering. Although there have been successful applications of CERR l dependence, it appears not to have become generally established for heavy ion or α scattering.

8.3 Strong channel coupling in ^{16}O scattering on ^{12}C at 330 MeV and 116 MeV

Channel coupling induces DPPs in the interaction between heavy ions that have similar features to the DPPs arising in the scattering of nucleons and other light ions. This suggests an underlying l dependence. We now present evidence for this in the case of ^{16}O scattering on ^{12}C at 330 MeV and 116 MeV. Ohkubo and Hirabayashi [150] showed how, for 330 MeV ^{16}O scattering from ^{12}C, the excitation of strongly excited states in both nuclei greatly modified the elastic scattering angular distribution in a way that explained some long-standing paradoxical features. Subsequently, the elastic channel S_l from the coupled channel calculations were inverted to reveal DPPs that had quite strong and well-established undulatory features [151]. The possibility that this represents an underlying l-dependent potential was not explored but it is likely, especially since there was no apparent relationship between the undulations in the imaginary term and the radial dependence of the form factors for the inelastic coupling.

Subsequently, Ohkubo and Hirabayashi [152] performed similar calculations on the same pair of nuclei at the much lower energy of 115.9 MeV (resulting in very interesting conclusions concerning rainbow scattering). The elastic channel S_l has been inverted and very strong undulations have been found [153]. The amplitude of the undulations, together with the smaller number of partial waves at 116 MeV compared with 330 MeV made it impossible to establish a unique inverted potential. Apparently

there are too few partial waves in this case to avoid the transparent potentials mentioned in sect. 7.2.

The undulations exhibited by the alternative inverted potentials shared strong family characteristics. To understand these, model calculations were carried out at 115.9 MeV in which a standard potential similar to the bare potential of ref. [152] was made artificially l-dependent and S_l from this l-dependent potential was inverted. The imposed l dependence was simple and in the form of added terms $v(r) \times f(l)$ or $w(r) \times f(l)$ where the $f(l)$ factor multiplying a real ($v(r)$) or imaginary ($w(r)$) terms is given by

$$f(l) = \frac{1}{1 + \exp((l^2 - \mathcal{L}^2)/\Delta^2)}\,. \tag{11}$$

The $v(r)$ and $w(r)$ factors each have a Woods-Saxon form with the same radius and diffusivity parameters as the corresponding real and imaginary l-independent terms. As a result, the l-dependent potentials essentially have a real or imaginary component that is renormalized for l less than $\mathcal{L}$, with a fairly sharp transition since Δ is quite small. The potential is unmodified for l substantially greater than $\mathcal{L}$. The value of $\mathcal{L}$ was chosen close to the value of l for which $|S_l| \sim \frac{1}{2}$. This sharp transition gives a form of l dependence very different from the more gradual form of refs. [136,137,140] of sect. 8.1. We would not expect such a simple parameterization to exactly reproduce the specific undulations, yet many of the general features, such as strong undulations in the surface region of the imaginary term, emerged. This shows again that it is quite possible to have a potential with distinct excursions into emissivity but for which $|S_l| \leq 1$ for all l, conforming to the unitarity limit.

Details are presented in ref. [153], but the conclusion is clear: strong coupling to states of both ^{16}O and ^{12}C induces a DPP with an l-independent representation having strong undulations. Thus, a representation in terms of smooth potentials must have significant l dependence. The nature of this l dependence is plausibly of a form distinguishing between partial waves above and below the region where $|S_l| \sim \frac{1}{2}$.

Very recently, this scattering has been fitted very well with an alternative model involving α-cluster exchange leading to explicit Majorana terms in both real and imaginary components, see sect. 3.2, and ref. [79]. The inclusion of parity dependence in the inversion has enabled the determination of the DPPs due to inelastic coupling. Hence, it is likely that in this case a full specification of the l dependence would includes both parity dependence and the form we have associated with coupling to inelastic excitations.

8.4 More general l-dependence in ^{16}O scattering

Since the excitation of cluster states contributes to the scattering of ^{16}O from ^{12}C, it must be presumed to play some part in scattering from heavier target nuclei. The scattering of ^{16}O from ^{28}Si at about 55 MeV exhibited enhanced backward angle scattering for which there has been no widely agreed explanation, see ref. [154] for references. In ref. [155] the angular distribution was fitted with model independent searching using spline functions. In the region of the strong absorption radius (SAR), about 9 fm, the spline fit agreed well with potentials of standard parameterized form cited in ref. [154]. However, the closer fit to the data found by the spline model led to a potential that deviated markedly from the other fits in the range 6–8 fm, a range still important for a precise fit. This deviation was, in effect, part of a strong undulation that was undefined at smaller internuclear separation. Subsequent spline function fits [156] for ^{16}O-^{12}C elastic scattering from 33 to 55 MeV, consistently revealed similar marked deviations from folding model potentials.

These results bring into focus the choice of representation: l-dependence or wavy potential? Possibly there is parity dependence due to alpha cluster exchange, but it is unlikely that the undulations reflect corrections to local density folding models. The wide angular range data does not yet have an agreed explanation in terms of reaction dynamics, but it is certain that l-independent smooth potentials are excluded.

There is indirect evidence for l dependence applying to ^{16}O scattering from the heavier ^{40}Ca target at $E_{\mathrm{c.m.}} = 37.5$ MeV. It points to the need for care in interpreting spline model fits, see ref. [157]. Spline model fitting revealed small amplitude ($\sim \pm 2$ MeV) undulations in the radial range a few fm within the SAR. These were well-determined, unlike the wide amplitude undulations of previous spline model fits cited in ref. [157]. A natural explanation is l dependence in the underlying potential. More precise angular distribution measurements would enable modern fitting techniques to make a more definitive determination.

9 Implications and applications

The l dependence of the OMP is of intrinsic interest, but how is it to be taken into account in reaction calculations?

9.1 Practical implementation of l dependence

The l dependence of the OMP is an inconvenience. It is not commonly an option offered by standard reaction codes that involve the application of optical potentials. One problem is the wide variety of possible l dependencies. Nevertheless, there are certain forms of l dependence that should certainly be available for use in reaction calculations.

1) The interaction of light ions with lower mass targets will, in general, be parity dependent. For nucleon scattering on ^{16}O, or lighter, parity dependence should not be omitted and is very large for a ^{4}He target. It is significant for α plus ^{12}C, of astrophysical significance.
2) The success of the CERR l (or J) dependence for α or ^{6}Li scattering implies that this form should be available for reaction calculations over the appropriate energy range.

Concerning point 1: For α-^{12}C scattering, it is the even parity potential that is relevant to the astrophysical S-factor, but a potential fitted l-independently will have been influenced by odd-parity partial waves [86]. Where exchange processes lead to parity dependence, such dependence can be omitted only when exchange is included explicitly. Section 8.1 referred to various other forms of l dependence arising from antisymmetrization.

Concerning point 2: If CERR l or J dependence were firmly established, that would be a significant extension of the optical model. If the plausible formal arguments for CERR, in ref. [142], were proven invalid, that would present an interesting challenge.

The other forms of angular momentum dependence which, together with dynamical non-locality, arise from channel coupling, present a problem: there exists no widely accepted parameterized form for inclusion in reaction codes. The natural solution would be to explicitly include the many processes which generate l dependence in the direct reaction calculations.

It is often stated, as in ref. [158], that there exist elastic scattering angular distributions that cannot be described by a mean-field optical potential. But the existence of cases where *smooth* mean-field OMPs do not work does not mean that potential models fail. In cases like that of ref. [158], angular distributions can be fitted when strong channel coupling is included. By means of S-matrix inversion, such coupling effects can always be represented within a potential model. The potential will probably be undulatory, implying the existence of an alternative representation in terms of l dependence, although the form of the l dependence might not be easy to identify. In ref. [158] the effect of coupling is very large, and of great interest; this is an extreme case of a general property.

9.2 Consequences of l dependence for folding models

Single folding calculations, based on theoretical nucleon potentials of the kind discussed in sect. 2.2, have been applied with some success [159] to the scattering of lighter composite nuclei. It is unclear how an l-dependent nucleon potential should be incorporated in such single folding calculations. To the extent that l dependence can be associated with calculable reaction processes, it is those reaction processes that should be incorporated into the scattering calculations. For example, if the coupling to giant resonance states of the target is a major source of l dependence for nucleon scattering, then the same processes must be presumed to affect the scattering of composite nuclei. More generally, processes that lead to l dependence for proton scattering presumably give rise to l dependence for composite projectiles.

9.3 Application of l dependence in direct reactions

The l-dependent extension of the nucleon OMP is relevant to the analysis of direct reactions. Reference [105] compares the angular distributions for the proton inelastic scattering to the 3^- state of ^{16}O calculated with both l-dependent and l-independent OMPs. There is a considerable difference in the angular distribution away from the maximum.

There is a problematic aspect concerning the application of l-dependent potentials in CRC calculations. It is likely that a major source of l dependence is the coupling of collective states or reaction channels to the elastic channel. While it is interesting to study the application of such potentials in CRC calculations, it is inappropriate to include the same channel coupling that contributes to the l dependence, together with the explicit inclusion of that l dependence, within a larger coupled channel calculation. This is one aspect of a general non-trivial question, that we do not pursue here: how to justify the application of a potential, adjusted to reproduce elastic scattering data, to other reactions, including fusion.

9.4 Establishing l-independence

The inconvenience of l-dependence is evident, so it is valid to ask how one could demonstrate that OMPs relevant to a specific case of elastic scattering are *not* l dependent.

For nucleons, the basic requirement is a complete set of elastic scattering data, *i.e.* precise angular distribution, analysing power and spin rotation parameter data covering an angular range out to 180°. Here "precise" is vague, but χ^2 per datum of around unity for data that is precise and of full angular range is the target; this represents a precision rarely attained. If data that are imprecise and do not cover the full angular range can be fitted with a radially smooth l-independent potential, that has no implications concerning l-dependence.

If model-independent fitting, with sufficient degrees of freedom, yields a potential with χ^2 per degree of freedom close to unity and is free of radial structure (undularity) then it is justifiable to claim that there is no l-dependence for that case. Undularity in the real component that can be directly related to structure, *e.g.* nuclear density maxima or minima, does not count. Otherwise, if a completely non-undulatory potential fits the data, then angular momentum dependence is not a property of the local OMP for that case.

10 Conclusions and discussion

The simplest possible nuclear reaction is elastic scattering: the ingoing and outgoing nuclei are the same. Arguably, if we don't understand elastic scattering, we cannot claim to understand nuclear reactions. It is therefore disconcerting that a general property of elastic scattering is widely disregarded. That property is the angular momentum dependence of the internuclear interaction. A conclusion of the results assembled here is that interaction potentials between nuclei scattering from each other depend upon the orbital angular momentum l of their relative motion.

There are several distinct forms of l dependence for which there are both different degrees of certainty and different implications. It can be considered certain that the interaction between nucleons and ^{4}He and even ^{16}O and also, for example, between ^{3}He and ^{4}He are parity dependent, and this should be taken into account in analyses of these cases. The l dependence of the imaginary potential of the CERR form has not been widely adopted. It would be a genuine contribution to our understanding of heavy ion interactions if the process behind CERR l dependence were firmly established or shown to be absent. In another category is the dynamically induced l dependence of the nucleon-nucleus potential. There are both phenomenological and theoretical arguments for this, and these arguments deserve to be either strengthened or disproved. The nucleon-nucleus interaction has a special status as being a positive energy continuation of the shell model potential, and also being a vital ingredient in the analysis of direct reactions, a subject of continuing interest [160].

Dynamically induced l dependence would have the status of a generic phenomenon if that between interpenetrating heavier ions such as ^{12}C and ^{16}O, as in sect. 8.3, were firmly established. Precision fits to data will, in general (where the angular distributions are not too smooth) reveal the need for a departure from local density model potentials. Only an unnecessarily restrictive form of OMP fails. What is missing is a "dictionary" for interpreting undulatory potentials in terms of specific l dependencies.

Precise and complete elastic scattering data can always be fitted; model independent fitting takes us from the situation where particular data cannot be fitted well to the situation where the same data is manifestly incomplete. In fact, as exemplified in the ^{3}He case discussed in sect. 5.4, the incompleteness of existing data is the major barrier to establishing phenomenologically that l dependence is a general property of nuclear interactions. Relatively complete high quality data exists for some cases so it is a shame that the full information contained of such data is rarely fully exploited in a systematic way. There is an understandable reluctance for "just fitting data", especially when such fits lead to strong undulations, refs. [96,97]. It is fortunate that Kepler did not feel that way about fitting Tycho Brahe's high quality planet-Sun scattering data.

The thrust of the present review is that there is information concerning nuclear reactions, that is seldom fully exploited, that could be extracted from elastic scattering data. In fact the data is seldom complete and absence of spin-rotation nucleon scattering data is a real problem [101]. Nevertheless, we know that the success of conventional folding models to fit existing data is incomplete as are present attempts [32] to reproduce the data with channel coupling effects. One conclusion from the results reviewed here is that the local density approximation, which underlies most folding model calculations, cannot lead to a complete description of elastic scattering. Concerning CRC calculations, it is now well established that the DPPs representing channel coupling are never proportional, as a function of r, to the bare potential. It follows that, by approximately improving the fit of a folding model potential to data, by means of a uniform renormalization, an opportunity to extract information about reaction dynamics is lost. A model independent additive term is far preferable and might well contain indications of l dependence and be identifiable with calculable DPPs.

Concerning the inclusion of l-dependence in direct reaction calculations: it might prove to be best to include within the calculation the processes that lead to l-dependence.

There are some firm theoretical predictions for l dependence for the scattering of heavier nuclei, as we noted in sect. 8.1. For the scattering of nucleons and certain light nuclei, there are *direct* predictions of parity dependence that are supported by experiment. The theoretical arguments for more general l dependence are less direct, apart from the relationship established between undularity and reaction coupling. Establishing more direct evidence remains a challenge. It should not be forgotten that it is when our favorite folding model *fails* to give precise fits that we stand to learn. Arguably, our understanding of nucleon-nucleus scattering is incomplete even at the most phenomenological level.

There have been two recurring themes in this review:

1) Precise fits to elastic scattering data are required, but most existing elastic scattering data sets are incomplete. Fitting such data may well require potentials possessing undularity, including radial regions in which the imaginary term is emissive. Potentials with this property are generated by certain channel couplings and it does *not* necessarily break the rigorous unitarity limit, $|S_{lj}| \leq 1$.
2) Quote from sect. 6: "The nucleus-to-nucleus variation of collectivity and transfer reaction strength must affect the OMP in ways that are absent from standard folding models. This is why, for example, the helion global OMP of ref. [5] requires a "local" OMP near the ^{40}Ca closed shell." The need to relate the OMP to nuclear structure has been implicit throughout this review. It is not a coincidence that Pang's "local" potential [5] was required near ^{40}Ca. Both collectivity and transfer strength depend on nuclear properties in a way that is not a part of most folding model theories.

Those two themes are both involved in the case of protons scattering from the doubly closed shell nucleus ^{40}Ca: the precise angular distribution data for 30.3 MeV proton of [161] and the relatively precise analysing power data for the same case of‘ [162] were the first data to be known to require an l-dependent OMP in order to fit the deep minimum near 140°. Could such measurements be made today?

I am grateful to Nicholas Keeley for producing publishable figures and for many helpful discussions over the years.

Data Availability Statement This manuscript has no associated data or the data will not be deposited. [Author's comment: No data was generated during the making of this review.]

References

1. P. Darriulat, G. Igo, H.G. Pugh, H.D. Holmgren, Phys. Rev. **137**, B315 (1965).
2. R.S. Mackintosh, arXiv:1705.07003v6 (2019).
3. A.J. Koning, J.P. Delaroche, Nucl. Phys. A **713**, 231 (2003).
4. W.W. Daehnick, J.D. Childs, Z. Vrcelj, Phys. Rev. C **21**, 2253 (1980).
5. D.Y. Pang, P. Roussel-Chomaz, H. Savajols, R.L. Varner, R. Wolski, Phys. Rev. C **79**, 024615 (2009).
6. T. Furumoto, K. Tsubakihara, S. Ebata, W. Horiuchi, Phys. Rev. C **99**, 034605 (2019).
7. R.S. Mackintosh, Eur. Phys. J. A **53**, 66 (2017).
8. H. Feshbach, C.E. Porter, V.F. Weisskopf, Phys. Rev. **96**, 448 (1954).
9. R.D. Woods, D.S. Saxon, Phys. Rev. **95**, 577 (1954).
10. L.C. Gomes, J.D. Walecka, V.F. Weisskopf, Ann. Phys. (N.Y.) **3**, 241 (1958).
11. H. Feshbach, Ann. Phys. **5**, 357 (1958).
12. H. Feshbach, Ann. Phys. **19**, 287 (1962).
13. J.S. Bell, E.J. Squires, Phys. Rev. Lett. **3**, 96 (1959).
14. J.P. Jeukenne, A. Lejeune, C. Mahaux, Phys. Rev. C **10**, 1391 (1974).
15. J.P. Jeukenne, A. Lejeune, C. Mahaux, Phys. Rev. C **15**, 10 (1977).
16. C. Mahaux, R. Sartor, *Advances in Nuclear Physics*, Vol. **20**, edited by J.W. Negele, E. Vogt (Plenum, New York, 1991) p. 1.
17. F.A. Brieva, J.R. Rook, Nucl. Phys. A **291**, 299 (1977).
18. F.A. Brieva, J.R. Rook, Nucl. Phys. A **291**, 317 (1977).
19. F.A. Brieva, J.R. Rook, Nucl. Phys. A **297**, 206 (1978).
20. C. Mahaux, G.R. Satchler, Nucl. Phys. A **560**, 5 (1993).
21. H. Guo, Y. Xu, H. Liang, Y. Han, Q. Shen, Phys. Rev. C **83**, 064618 (2011).
22. K. Wildermuth, Y.C. Tang, *A Unified Theory of the Nucleus* (Vieweg, Braunschweig, 1977).
23. P. Descouvement, M. Dufour, in *Clusters in Nuclei*, Vol. **2**, edited by C. Beck, Lect. Notes Phys., Vol. **848** (Springer, 2012) p. 1.
24. Y. Suzuki, R.G. Lovas, K. Yabana, K. Varga, *Structure and Reactions of Light Exotic Nuclei* (Taylor and Francis, London, 2003).
25. C.L. Rao, M. Reeves, G.R. Satchler, Nucl. Phys. A **207**, 182 (1973).
26. C.A. Coulter, G.R. Satchler, Nucl. Phys. A **293**, 269 (1977).
27. G.H. Rawitscher, Nucl. Phys. A **475**, 519 (1987).
28. N.K. Glendenning, D.L. Hendrie, O.N. Jarvis, Phys. Lett. B **26**, 131 (1968).
29. R.S. Mackintosh, Nucl. Phys. A **164**, 398 (1971).
30. G.R. Satchler, *Direct Nuclear Reactions* (Clarendon Press, Oxford, 1983).
31. R.S. Mackintosh, N. Keeley, Phys. Rev. C **81**, 034612 (2010).
32. R.S. Mackintosh, N. Keeley, Phys. Rev. C **85**, 064603 (2012).
33. N. Keeley, R.S. Mackintosh, Phys. Rev. C **97**, 014605 (2018).
34. R.S. Mackintosh, N. Keeley, Phys. Rev. C **98**, 069901(E) (2018).
35. N. Keeley, R.S. Mackintosh, Phys. Rev. C **99**, 034614 (2019).
36. R.S. Mackintosh, N. Keeley, Phys. Rev. C **90**, 044601 (2014).
37. E. Bauge, J.P. Delaroche, M. Girod, Phys. Rev. C **58**, 1118 (1998).
38. E. Bauge, J.P. Delaroche, M. Girod, Phys. Rev. C **63**, 024607 (2001).
39. N. Vinh Mau, *Microscopic Optical Potentials*, edited by H.V. von Geramb, Lecture Notes in Physics, Vol. **89** (Springer Verlag, New York, 1979) p. 104.
40. N. Vinh Mau, A. Boussy, Nucl. Phys. A **257**, 189 (1976).
41. F. Osterfeld, J. Wambach, V.A. Madsen, Phys. Rev. C **23**, 179 (1981).
42. J. Wambach, V.K. Mishra, Li Chu-Hsia, Nucl. Phys. A **380**, 285 (1982).
43. V.A. Madsen, P. Osterfeld, Phys. Rev. C **39**, 1215 (1989).
44. M. Pignanelli, H.V. von Geramb, R. DeLeo, Phys. Rev. C **24**, 369 (1981).
45. J.P. Delaroche, M.S. Islam, R.W. Finlay, Phys. Rev. C **33**, 1826 (1986).
46. G.M. Honoré, W. Tornow, C.R. Howell, R.S. Pedroni, R.C. Byrd, R.L. Walter, J.P. Delaroche, Phys. Rev. C **33**, 1129 (1986).
47. C. Mahaux, H. Weidenmüller, *Shell-Model Approach to Nuclear Reactions* (North Holland Publishing Co., Amsterdam, 1969).
48. N. Austern, Phys. Rev. B **137**, 752 (1965).
49. N. Keeley, R.S. Mackintosh, Phys. Rev. C **90**, 044602 (2014).
50. B. Buck, Phys. Rev. **130**, 712 (1963).
51. F.G. Perey, Phys. Rev. **131**, 745 (1963).
52. R.S. Mackintosh, Phys. Lett. B **44**, 437 (1973).
53. R.S. Mackintosh, Nucl. Phys. A **230**, 195 (1974).
54. A.M. Kobos, R.S. Mackintosh, Phys. Lett. B **62**, 127 (1976).
55. R.S. Mackintosh, N. Keeley, Phys. Rev. C **98**, 024624 (2018).
56. R.S. Mackintosh, A.M. Kobos, J. Phys. G: Nucl. Part. Phys. **5**, 359 (1979).
57. M.A. Franey, P.J. Ellis, Phys. Rev. C **23**, 787 (1981).
58. I.J. Thompson, Comput. Phys. Rep. **7**, 167 (1988).
59. L.W. Owen, G.R. Satchler, Phys. Rev. Lett. **25**, 1720 (1970).
60. B.Z. Georgiev, R.S. Mackintosh, Phys. Lett. B **73**, 250 (1978).
61. B.T. Kim, M.C. Kyum, S.W. Hong, M.H. Park, T. Udagawa, Comput. Phys. Commun. **71**, 150 (1992).
62. B.T. Kim, T. Udagawa, Phys. Rev. C **42**, 1147 (1990).
63. F.G. Perey, B. Buck, Nucl. Phys. **32**, 353 (1962).
64. R.S. Mackintosh, S.G. Cooper, J. Phys. G: Nucl. Part. Phys. **23**, 565 (1997).

65. D. Lukaszek, G.H. Rawitscher, Phys. Rev. C **50**, 968 (1994).
66. C.H. Johnson, C. Mahaux, Phys. Rev. C **38**, 2589 (1988).
67. M.A. Nagarajan, C. Mahaux, G.R. Satchler, Phys. Rev. Lett. **54**, 1136 (1985).
68. S. Ait-Tahar, R.S. Mackintosh, M.A. Russell, J. Phys. G: Nucl. Part. Phys. **21**, 577 (1995).
69. R.S. Mackintosh, *Inverse scattering: Applications in nuclear physics* (Scholarpedia, 2012).
70. D. Baye, Nucl. Phys. A **460**, 581 (1986).
71. F.K. Vosniakos, N.E. Davison, W.R. Falk, O. Abou-Zeid, S.P. Kwan, Nucl. Phys. A **332**, 157 (1979).
72. R.S. Mackintosh, Nucl. Phys. A **742**, 3 (2004).
73. R.S. Mackintosh, S.G. Cooper, Nucl. Phys. A **589**, 377 (1995).
74. S.G. Cooper, R.S. Mackintosh, Nucl. Phys. A **592**, 338 (1995).
75. V.I. Kukulin, R.S. Mackintosh, J. Phys. G: Nucl. Part. Phys. **30**, R1 (2004).
76. F. Michel, G. Reidemeister, Z. Phys. A **333**, 331 (1989).
77. S.G. Cooper, R.S. Mackintosh, Z. Phys. A **337**, 357 (1990).
78. N.N.T. Phuc, N.H. Phuc, D.T. Khoa, Phys. Rev. C **98**, 024613 (2018).
79. N.N.T. Phuc, R.S. Mackintosh, N.H. Phuc, D.T. Khoa, in preparation.
80. D.R. Thompson, Y.C. Tang, Phys. Rev. C **4**, 306 (1971).
81. D.R. Thompson, Y.C. Tang, R.E. Brown, Phys. Rev. C **5**, 1939 (1972).
82. G.W. Greenlees, W. Makofske, Y.C. Tang, D.R. Thompson, Phys. Rev. C **6**, 2057 (1972).
83. S.G. Cooper, R.S. Mackintosh, Phys. Rev. C **54**, 3133 (1996).
84. S.G. Cooper, Nucl. Phys. A **618**, 87 (1997).
85. H. Heiberg-Andersen, R.S. Mackintosh, J.S. Vaagen, Nucl. Phys. A **713**, 63 (2003).
86. S.G. Cooper, R.S. Mackintosh, Nucl. Phys. A **517**, 285 (1990).
87. A.A. Ioannides, R.S. Mackintosh, Nucl. Phys. A **438**, 354 (1985).
88. R.S. Mackintosh, A.A. Ioannides, in *Advanced Methods in the Analysis of Nuclear Scattering Data*, Lect. Notes Phys., Vol. **236** (Springer Verlag, Berlin, 1985) p. 283.
89. R.S. Mackintosh, A.M. Kobos, Phys. Lett. B **116**, 95 (1982).
90. A.A. Ioannides, R.S. Mackintosh, Nucl. Phys. A **467**, 482 (1987).
91. S.G. Cooper, R.S. Mackintosh, Inverse Probl. **5**, 707 (1989).
92. R.S. Mackintosh, arXiv:1205.0468 (2012).
93. R.S. Mackintosh, A.M. Kobos, Phys. Lett. B **116**, 95 (1982).
94. R.S. Mackintosh, Scholarpedia **7**, 12032 (2012) `https://doi.org/10.4249/scholarpea.12032`.
95. S.G. Cooper, *Notes for Imago users*, Open University report (1999) unpublished, available upon request.
96. M. Ermer, H. Clement, P. Grabmayr, G.J. Wagner, L. Friedrich, E. Huttel, Phys. Lett. B **188**, 17 (1987).
97. M. Ermer, H. Clement, G. Holetzke, W. Kabitzke, G. Graw, R. Hertenberger, H. Kader, F. Merz, P. Schiemenz, Nucl. Phys. A **533**, 71 (1991).
98. A.M. Kobos, R.S. Mackintosh, Ann. Phys. (N.Y.) **123**, 296 (1979).
99. R. Alarcon, J. Rapaport, R.W. Finlay, Nucl. Phys. A **462**, 413 (1987).
100. R.E. Shamu, J. Barnes, S.M. Ferguson, G. Haouat, J. Lachkat, J. Phys. G: Nucl. Part. Phys. **17**, 525 (1991).
101. A.M. Kobos, R.S. Mackintosh, J.R. Rook, Nucl. Phys. A **389**, 205 (1982).
102. R.S. Mackintosh, J. Phys. G: Nucl. Part. Phys. **5**, 1587 (1979).
103. R.S. Mackintosh, L.A. Cordero-L., Phys. Lett B **68**, 213 (1977).
104. A.M. Kobos, R.S. Mackintosh, J. Phys. G: Nucl. Part. Phys. **5**, 97 (1979).
105. A.M. Kobos, R.S. Mackintosh, Acta Phys. Pol. B **12**, 1029 (1981).
106. R.S. Mackintosh, unpublished (2016) postscript files available on request.
107. R.S.Mackintosh, unpublished (1978) scanned copy available on request.
108. Y.-W. Lui, O. Karban, S. Roman, R.K. Bhowmik, J.M. Nelson, E.C. Pollacco, Nucl. Phys. A **333**, 205 (1980).
109. M.E. Cage, D.L. Clough, A.J. Cole, J.B.A England, G.J. Pyle, P.M. Rolph, L.H. Watson, D.H. Worledge, Nucl. Phys. A **183**, 449 (1972).
110. R.S. Mackintosh, S.G. Cooper, A.A. Ioannides, Nucl. Phys. A **476**, 287 (1987).
111. R.S. Mackintosh, K. Rusek, Phys. Rev. C **67**, 034607 (2003).
112. N. Keeley, R.S. Mackintosh, Phys. Rev. C **83**, 044608 (2011).
113. F. Skaza *et al.*, Phys. Lett. B **619**, 82 (2005).
114. R.S. Mackintosh, N. Keeley, Phys. Rev. C **83**, 057601 (2011).
115. R.S. Mackintosh, N. Keeley, Phys. Rev. C **76**, 024601 (2007).
116. D.Y. Pang, R.S. Mackintosh, Phys. Rev. C **84**, 064611 (2011).
117. G. Marquíinez-Durán, N. Keeley, K.W. Kemper, R.S. Mackintosh, I. Martel, K. Rusek, A.M. Sánchez-Benítez, Phys. Rev. C **95**, 024602 (2017).
118. A.A. Ioannides, R.S. Mackintosh, Phys. Lett. B **169**, 113 (1986).
119. R.S. Mackintosh, D.Y. Pang, Phys. Rev. C **86**, 047602 (2012).
120. N. Keeley, R.S. Mackintosh, C. Beck, Nucl. Phys. A **834**, 792c (2010).
121. R.S. Mackintosh, D.Y. Pang, Phys. Rev. C **88**, 014608 (2013).
122. N. Keeley, R.S. Mackintosh, Phys. Rev. C **77**, 054603 (2008).
123. R.S. Mackintosh, A.A. Ioannides, S.G. Cooper, Nucl. Phys. A **483**, 173 (1988).
124. R.S. Mackintosh, A.A. Ioannides, S.G. Cooper, Nucl. Phys. A **483**, 195 (1988).
125. R.S. Mackintosh, S.G. Cooper, Nucl. Phys. A **494**, 123 (1989).
126. S.G. Cooper, R.S. Mackintosh, Nucl. Phys. A **511**, 29 (1990).
127. R. Crespo, R.C. Johnson, J.A. Tostevin, R.S. Mackintosh, S.G. Cooper, Phys. Rev. C **49**, 1091 (1994).
128. F.G. Perey, in *Direct interactions and nuclear reaction mechanisms*, edited by E. Clemental, C. Villi (Gordon and Breach, New York, 1963).
129. R.S. Mackintosh, unpublished preprint, available.

130. E.E. Gross, R.H. Bassel, L.N. Blumberg, B.J. Morton, A. van der Woude, A. Zucker, Nucl. Phys. A **102**, 673 (1967).
131. D.J. Horen, C.H. Johnson, A.D. MacKellar, Phys. Lett. B **161**, 217 (1085).
132. D.J. Horen, C.H. Johnson, J.L. Fowler, A.D. MacKellar, B. Castel, Phys. Rev. C **34**, 429 (1986).
133. C.H. Johnson, D.J. Horen, C. Mahaux, Phys. Rev. C **36**, 2252 (1987).
134. C.H. Johnson, R.R. Winters, Phys. Rev. C **37**, 2340 (1988).
135. J.-P. Jeukenne, C.H. Johnson, C. Mahaux, Phys. Rev. C **38**, 2573 (1988).
136. T. Wada, H. Horiuchi, Prog. Theor. Phys. **80**, 488 (1988).
137. T. Wada, H. Horiuchi, Prog. Theor. Phys. **80**, 502 (1988).
138. H. Horiuchi, in *Proceedings of the International Conference on Clustering Aspects of Nuclear Structure and Nuclear Reactions (Chester, 1984)*, edited by J.S. Lilley, M.A. Nagarajan (Reidel, Dordrecht, 1984) p. 35.
139. S. Ait-Tahar, R.S. Mackintosh, S.G. Cooper, T. Wada, Nucl. Phys. A **562**, 101 (1993).
140. Y. Kondo, B.A. Robson, R. Smith, Phys. Lett. B **227**, 310 (1989).
141. S. Ait-Tahar, S.G. Cooper, R.S. Mackintosh, Nucl. Phys. A **542**, 499 (1992).
142. R.A. Chatwin, J.S. Eck, D. Robson, A. Richter, Phys. Rev. C **1**, 795 (1970).
143. A.E. Bisson, R.H. Davis, Phys. Rev. Lett. **22**, 542 (1969).
144. A.E. Bisson, K.A. Eberhard, R.H. Davis, Phys. Rev. C **1**, 539 (1970).
145. C. Gao, G. He, Phys. Lett. B **282**, 16 (1992).
146. S. Ait-Tahar, R.S. Mackintosh, S.G. Cooper, Nucl. Phys. A **561**, 285 (1993).
147. H. Bohn, K.A. Eberhart, R. Vandenbosch, K.G. Bernhardt, R. Bangert, Y.-d. Chan, Phys. Rev. C **16**, 665 (1977).
148. D.E. Trcka, A.D. Frawley, K.W. Kemper, D. Robson, J.D. Fox, E.G. Myers, Phys. Rev. C **41**, 2134 (1990).
149. E.L. Reber, K.W. Kemper, P.V. Green, P.L. Kerr, A.J. Mendez, E.G. Myers, B.G. Schmidt, Phys. Rev. C **49**, R1 (1994).
150. S. Ohkubo, Y. Hirabayashi, Phys. Rev. C **89**, 051601 (2014).
151. R.S. Mackintosh, Y. Hirabayashi, S. Ohkubo, Phys. Rev. C **91**, 024616 (2015).
152. S. Ohkubo, Y. Hirabayashi, Phys. Rev. C **89**, 061601 (2014).
153. R.S. Mackintosh, Phys. Rev. C **94**, 034602 (2016).
154. S.Y. Lee, Nucl. Phys. A **311**, 518 (1978).
155. R.S. Mackintosh, A.M. Kobos, Phys. Lett. B **92**, 59 (1980).
156. A.M. Kobos, G.R. Satchler, R.S. Mackintosh, Nucl. Phys. A **395**, 248 (1983).
157. A.M. Kobos, R.S. Mackintosh, Phys. Rev. C **26**, 1766 (1982).
158. S. Ohkubo, Y. Hirabayashi, A.A. Ogloblin, Phys. Rev. C **92**, 051601 (2015).
159. D.Y. Pang, Y.L. Ye, F.R. Xu, Phys. Rev. C **83**, 064619 (2011).
160. F.M. Nunes, A. Lovell, A. Ross, L.J. Titus, R.J. Charity, W.H. Dickhoff, M.H. Mahzoon, J. Sarich, S.M. Wild, arXiv:1509.047001.
161. B.W. Ridley, J.F. Turner, Nucl. Phys. **58**, 497 (1964).
162. V. Hnizdo, O. Karban, J. Lowe, G.W. Greenlees, W. Makofske, Phys. Rev. C **3**, 1560 (1971).

Raymond Mackintosh received BSc and MSc degrees in physics from the University of Auckland, New Zealand. Following the award of a Fulbright Fellowship, he obtained his PhD in nuclear theory at the University of California, Berkeley, under Norman Glendenning. After post doctoral positions at the ANU Canberra Australia, Oxford University UK and Daresbury Laboratory UK, he became a faculty member of the Open University in Milton Keynes, UK, where he is currently Emeritus Professor of physics.